PHYSICAL MODEL TESTING OF NEGRIL BREAKWATER IN JAMAICA

BY

ROLANDO GARCIA, NOBUHISA KOBAYASHI, REBECCA QUAN,

HEATHER WEITZNER AND BURAK AYDOGAN

MODEL TESTING REPORT NO. CACR-2013
DECEMBER 2013

CENTER FOR APPLIED COASTAL RESEARCH

Ocean Engineering Laboratory
University of Delaware
Newark, Delaware 19716

ACKNOWLEDGEMENT

This experiment has been supported by CEAC Solutions Co., Ltd. in Jamaica.

The authors would like to thank Messrs. Chris Burgess, Carlnenus Johnson, Mark Richards, Kris Henry, and Allan Hamilton who participated in the physical model testing of the Negril breakwater in Jamaica during December 4, 5 and 6 in 2013.

Table of Contents

APPENDIX A: Results of numerical model for specification of testing conditions in physical model.

APPENDIX B: Stones measurements for physical model.

APPENDIX C: Measured profiles of the physical model.

APPENDIX D: Results of hydrodynamic measurements of the physical model.

APPENDIX E: Physical model photographs and laser scan for damage estimation.

APPENDIX F: Results of numerical model for recommended design

List of Tables

List of Figures

1 SUMMARY AND RECOMMENDATIONS

1.1 SUMMARY

Physical model testing at the Center for Applied Coastal Research was conducted to optimize the cross section of the Negril rubble mound breakwater in Jamaica which was designed by CEAC Solutions Co., Ltd. in Jamaica.

Before the physical model testing in December 2013, the designed cross section was evaluated using the latest empirical formulas for armor stability and wave transmission on detached low-crested breakwaters. The cross-shore numerical model CSHORE developed by the Center for Applied Coastal Research with funding from the U.S. Army Coastal and Hydraulics Laboratory was also applied to predict the damage progression of the breakwater cross section under design wave conditions. These evaluations indicated the sufficient stability of the landward primary armor layer of 7 to 13 ton stones and the seaward secondary armor layer of 5 to 9 ton stones. The armor layer of 3 ton stones was predicted to suffer noticeable stone displacement. The toe (and base) consisting of 0.3 to 0.6 ton stones was computed to be less stable than the armor layers of 5 to 13 ton stones. On the other hand, the predicted wave transmission coefficient was in the range of 0.3 to 0.7, depending on the offshore significant wave height of 5 to 8 m, the spectral peak period of 11.1 to 12.4 s, and the water level of -0.5 to 0.5 m relative to the crest elevation of the southern breakwater. Since the wave energy is proportional to the wave height squared, the transmitted wave energy was predicted to be less than one half of the incident wave energy. The evaluated results for the Negril breakwater were used to devise necessary physical model testing and optimize the breakwater cross section with more confidence where the errors associated with the empirical formulas and numerical model are within a factor of about 2 (100%).

The experiment was conducted in a wave tank that was 30 m long, 2.5 m wide, and 1.5 m high. A dividing wall in the middle of the wave tank reduced the amount of fine sand used for the beach and seiching development in the wave tank. The experimental facilities were developed by Figlus et al. (2011). The model testing was performed in a 23 m long and 1.15 m wide flume. A piston-type wave maker in water depth of approximately 0.8 m generated a 400 s burst of irregular waves corresponding to a TMA spectrum. The length scale of the model experiment based on Froude similitude was selected to be 1/36 (1 m in model corresponds to 36 m in the prototype) in view of the wave maker capability for generating nonbreaking irregular waves with the significant wave height of 17.5 cm (6.3 m in prototype) and the spectral peak period of 2.0 – 2.6 s (12.0 – 15.6 s in prototype) in water depth of 0.8 m (28.8 m in prototype). The corresponding time scale was $1/\sqrt{36} = 1/6$ (400 s in model corresponds to 2,400 s = 2/3 hr in prototype). Six capacitance wave gauges were used to measure the cross-shore variation of the free surface elevation. Two acoustic Doppler velocimeters (ADV) were used to measure fluid velocities at locations seaward and landward of the breakwater. A laser line scanner mounted on a motorized cart was used to measure three-dimensional bathymetry after lowering the water level. An array of three submerged ultrasonic transducers measured the underwater portion of the beach. Two fixed

video cameras were installed to record the stone movement during the 400-s burst from the side and top of the flume. The number of dislodged stones (colored to differentiate the primary and secondary armor stones and toe stones) was counted after each 400-s burst.

Preparatory tests were conducted before the visit by the Jamaican delegation during December 4, 5, and 6 in 2013. First, the wave generation and transformation on the beach were examined to ensure the reproduction of the target wave conditions in the absence of the breakwater. The water depth in the flume was 80 or 82 cm (2 cm difference in model corresponds to 72 cm difference in prototype) to assess the effect of the still water depth above the breakwater crest on the armor stability. The incident significant wave height was approximately 17.5 cm but the waves at the breakwater location in the water depth of about 12 cm (4.3 m in the prototype) were broken waves whose significant wave height was limited by the shallow water depth. The spectral wave period was 2.0 or 2.6 s to assess the effect of the wave period on the armor stability where low-frequency waves generated in the surf zone may increase the representative wave period for the armor stability analysis. After the reproduction of the target wave conditions and water level was confirmed, the model rubble mound based on the designed cross section was constructed at the cross-shore location in the water depth of about 12 cm below the still water level. The breakwater crest height above the local bottom was 9.3 cm. The primary and secondary armor stones were observed to be stable (apart from a few stones placed in unstable positions) during 1 hr (6 hr in prototype) wave action for the two different water depths of 80 and 82 cm and the two different wave periods of 2.0 and 2.6 s. The toe stones were less stable as predicted by the numerical model CSHORE but the dislodgement of a number of the toe stones did not affect the stability of the primary and secondary armor stones. The wave transmission coefficient defined as the ratio of the significant wave heights measured landward and seaward of the breakwater was about 0.6 for the still water level near the breakwater crest.

During the visit of the Jamaican delegation, one of the preparatory tests was repeated to demonstrate the stability of the primary and secondary armor stones and the dislodgement of a number of the toe stones. The empirical, numerical and experimental results described above were presented for the discussion of the simplification (and construction cost reduction) of the breakwater cross section. The separation of the primary and secondary armor layers was abandoned. The armor layer of the 5 to 9 ton stones was constructed and tested to confirm its stability. The armor layer of 5 to 7 ton stones and the armor layer of 7 to 9 ton stones constructed side by side in the wave flume were tested to confirm the reduced stability of the 5 to 7 ton stone armor layer in comparison to the 7 to 9 ton stone armor layer under different water levels. The increase of the water level increased the water depth in front of the breakwater and the depth-limited wave height impinging on the armor stones. The increase of the water level also increased the water depth above the breakwater crest and the wave transmission coefficient. However, the increased water depth cushioned the impact of the depth-limited broken waves on the armor stones. As a result, the armor stability was observed to be insensitive to the water level for the Negril breakwater.

The wide and shallow shelf offshore of the Negril breakwater was not simulated in this physical model testing. The cross-shore distance for breaking wave energy dissipation was shorter than that required by the geometric similitude. The breaker parameter γ defined as the ratio between the significant wave height and the still water depth in front of the breakwater was larger in the model testing than that computed by CSHORE for the prototype conditions. On the other hand, the densities of the armor stones in the model testing were approximately 3.0 ton/m^3, whereas the densities of the prototype stones may be 2.5 ton/m^3 or slightly larger. The effects of the differences of the γ values and the stone densities tend to cancel out on the basis of the stability number which is regarded to represent the ratio between the wave force acting on a stone and the submerged stone weight. The stability number was approximately the same in the model and prototype. The stability of the prototype 5 to 9 ton stones with the density of 2.5 ton/m^3 was confirmed using the numerical model CSHORE with the prototype bathymetry.

1.2 RECOMMENDATIONS

The summary above is based on the subsequent chapters in the report. The empirical formulas and the numerical model CSHORE are explained later to provide the background information.

For the protection of the seaward slope, crest, and landward slope of the breakwater, an armor layer of two-stone thickness consisting of 5 to 9 ton stones will be sufficient. The wider gradation of 5 to 13 ton stones will also be sufficient if larger stones can be placed in interlocking manners.

For the toe protection and the underlayer (base) below the armor layer, it is safer to replace the proposed 0.3 to 0.6 ton stones by 0.5 to 0.9 ton stones because of the noticeable stone dislodgement observed during the model testing. In addition, the toe stone stability will be affected by longshore currents that were not considered in this study. Shore Protection Manual (1984) recommended that the toe stone mass and the underlayer stone mass should be one-tenth (1/10) of the armor stone mass for a rubble-mound cross section with wave exposure on both seaward and landward sides. The underlayer stones should be sufficiently large in comparison to the gaps among the armor stones to avoid filtering through the gaps. A quarry may produce 0.9 to 5 ton stones. These stones may be used as the toe and underlayer stones if these stones can be placed in such a way that the deviation between the designed and constructed cross sections of the breakwater is small.

As for the wave transmission over and through the breakwater, this study was limited mostly to storm waves. The breakwater will reduce the incident storm wave energy more than 50% if the still water depth above the breakwater crest is small relative to the incident significant wave height. For sufficiently small waves under normal conditions, the incident waves may not break on the breakwater crest and most of the incident wave energy will be transmitted landward. Submerged breakwaters are widely used for shoreline protection in Japan because of their aesthetics and effectiveness in triggering large wave breaking without eliminating the landward flow of water, which may be important for water quality and ecological considerations (Artificial Reef Design Manual 2004).

Finally, it is recommended to monitor the performance of the constructed breakwaters. Field data will be essential for the sustainable development of the coastal area affected by the Negril breakwater construction.

2 BACKGROUND INFORMATION

2.1 EMPIRICAL FORMULAS

Empirical formulas for the prediction of the wave transmission coefficient became more complex and accurate as the number of laboratory data sets increased. Goda and Ahrens (2008) combined formulas for wave transmission over and through low-crest structures and calibrated the combined formula using 14 data sets consisting of 851 data points (measured wave transmission coefficients). Tomasicchio et al. (2011) recalibrated the formula of Goda and Ahrens (2008) using 33 data sets consisting of 3300 data points. The agreement between the measured and predicted transmission coefficients was within a factor of about 2 probably because of the differences of the experimental setups and measurements. The formula of Tomasicchio et al. (2011) was used in this study but the predicted wave transmission coefficient may not be very accurate.

Empirical formulas for armor stability on the seaward slope of a rubble mound structure with no or little wave overtopping are well known and included in Shore Protection Manual (1984) and Coastal Engineering Manual (2003). For a stone armor layer, damage is normally expressed by damage $S_p = \left(A_e/{D_{n50}}^2\right)$ where A_e = eroded cross-section area and $D_{n50} = (M_{50}/\rho_s)^{1/3}$ with M_{50} = median stone mass and ρ_s = stone density. The damage S_p may be interpreted as the number of stones removed from the eroded area with an alongshore width of D_{n50}. It is difficult to measure the eroded area accurately if S_p is small. Alternatively, the damage S_v based on the number of dislodged stones was proposed by Vidal et al. (1992) where S_v is normally slightly larger than S_p because some of the dislodged stones may be deposited in the eroded area. The value of S_v is regarded to be more reliable if the number of dislodged stones is small as was the case in this experiment. The degree of stone stability is normally represented by the stability number $N_s = H_s/[(\rho_s/\rho) - 1]$ with H_s = significant wave height in front of the breakwater and ρ = water density.

For low-crested stone breakwaters, the stability of stones on the seaward slope, crest, and landward slope depends on the breakwater freeboard F (negative for submerged breakwaters) which influences the degree of wave overtopping and transmission. Vidal et al. (1992) measured damage on a low-crested stone structure in a wave basin experiment and expressed the stability number N_s for the specified damage level as a function of the normalized freeboard F/D_{n50} for the breakwater trunk. The analyzed data for the breakwater head was presented in Vidal et al. (1995). Kramer and Burcharth (2003) conducted a wave basin experiment to investigate the stability of low-crested breakwaters in shallow water under directional random waves. The analyzed data were compared with the data by Vidal et al. (1992, 1995) and the 1995 Delft data. The stability number N_s for the initiation of damage (S_v = 0.5 – 1.0) was plotted as a function of F/D_{n50} where N_s was the minimum in the vicinity of $(F/D_{n50}) = 0$ and $N_s > 1$ for all data points. The lower bound of N_s was expressed as a function of F/D_{n50}. The lower bound formula was extrapolated to depth-limited breaking waves with $H_s = \gamma h$ with γ = 0.6 and h = still water depth. The accuracy of this extrapolation is uncertain because the data sets did not include the

breakwater situated well inside the surf zone and the approximation of $H_s = \gamma h$ is regarded to be crude by those who analyze the cross-shore wave transformation in the surf zone. Burcharth et al. (2006) described the data and formulas for the structural stability of detached low-crested breakwaters. Wide-crested submerged breakwaters in Japan were described in Artificial Reef Design Manual (2004). In short, our understanding of low-crested breakwaters has improved but site-specific physical model testing is essential for breakwater design.

2.2 NUMERICAL MODEL CSHORE

The hydrodynamic model in CSHORE based on the time-averaged continuity, momentum and energy equations predicts the cross-shore variations of the mean and standard deviation (related to the intensity of wave motion) of the free surface elevation and depth-averaged horizontal velocity. Kobayashi et al. (2007) conducted a laboratory experiment on irregular breaking wave transmission over a wide-crested submerged porous breakwater for the calibration and verification of the hydrodynamic model. Kobayashi et al. (2010) extended the hydrodynamic model to the intermittently wet and dry zone above the still water level in order to predict irregular wave runup and overtopping on a permeable structure. Damage progression of a stone armor layer was predicted by modifying a formula for bed load on sand beaches. The damage progression model was compared with the three tests by Melby and Kobayashi (1998) which lasted up to 28.5 hr. The eroded area of the damaged armor layer on a traditional stone breakwater with little wave overtopping was predicted within a factor of 2.

Kobayashi et al. (2013) extended the hydrodynamic model to the zone of wave transmission landward of a low-crested porous breakwater. The extended model was compared with 148 tests by Ahrens (1989) for a reef breakwater with a narrow crest at or above the still water level where the narrow crest was lowered by wave action. The model was also compared with an experiment by Ota et al. (2006) for a wide-crested submerged breakwater whose crest height increased during wave action of 20 hours. The damage, crest height, and wave transmission coefficient were predicted reasonably well. Garcia and Kobayashi (2013) compared the low-crested breakwater model with 35 tests by Vidal and Mansard (1995) and 69 tests by Kramer and Burcharth (2002). The agreement for the damage and wave transmission coefficient was within a factor of about 2 as before. The low-crested breakwaters in these wave basin experiments included the semicircular head whose diameter was equal to the base width of the trunk section. Garcia and Kobayashi (2013) showed that damage on the front head could be predicted as damage on the seaward slope of the trunk. Damage on the emerged back head was similar to damage on the crest and landward slope of the corresponding trunk section. The submerged back head was more stable than the trunk crest and landward slope. This implies that the head of the Negril breakwater, which was not examined in this study, may be as stable as the trunk section examined in this study if a conventional semicircular head is adopted.

2.3 REFERENCES

Ahrens, J.P. (1989). "Stability of reef breakwaters." J. Waterway, Port, Coastal, Ocean Eng., 115(2), 221-234.

Artificial Reef Design Manual. (2004). Ministry of Land, Infrastructure, Transport and Tourism, River Division, Coastal Branch, Tokyo, Japan (in Japanese).

Burcharth, H.F., Kramer, M., Lamberti, A., Zanuttigh, B. (2006). "Structural stability of detached low crested breakwaters." Coastal Eng., 53, 381-394.

Coastal Engineering Manual. (2003). Coastal and Hydraulics Lab., U.S. Army Engineer Research and Development Center, Vicksburg, MS.

Figlus, J., Kobayashi, N., Gralher, C., and Iranzo, V. (2011). "Wave overtopping and overwash of dunes." J. Waterway, Port, Coastal, Ocean Eng., 137(1), 26-33.

Garcia, R., and Kobayashi, N. (2014). "Damage variations on low-crested breakwaters." Proc. 34th Coastal Engineering Conf. (submitted).

Goda, Y., and Ahrens, J.P. (2008). "New formulation of wave transmission over and through low-crested structures." Proc. 31st Coastal Engineering Conf., World Scientific, Singapore, 3530-3541.

Kobayashi, N., Farhadzadeh, A., and Melby, J.A. (2010). "Wave overtopping and damage progression of stone armor layer." J. Waterway, Port, Coastal, Ocean Eng., 136(5), 257-265.

Kobayashi, N., Meigs, L.E., Ota, T., and Melby, J.A. (2007). "Irregular breaking wave transmission over submerged porous breakwater." J. Waterway, Port, Coastal, Ocean Eng., 133(2), 104-116.

Kobayashi, N., Pietropaolo, J., and Melby, J.A. (2013). "Deformation of reef breakwaters and wave transmission." J. Waterway, Port, Coastal, Ocean Eng., 139(4), 336-340.

Kramer, M., and Burcharth, H. (2004). "Wave basin experiment final form, 3-D stability tests at AAU." Report of DELOS EVK-CT-2000-0004, www.delos.unibo.it .

Kramer, M., and Burcharth, H. (2003). "Stability of low-crested breakwaters in shallow water short crested waves." Proc. Coastal Structures 2003, ASCE, Reston, VA, 137-149.

Melby, J.A., and Kobayashi, N. (1998). "Progression and variability of damage on rubble mound breakwaters." J. Waterway, Port, Coastal, Ocean Eng., 124(6), 286-294.

Ota, T., Kobayashi, N., and Kimura, A. (2006). "Irregular wave transformation over deforming submerged breakwaters." Proc. 30th Coastal Engineering Conf., World Scientific, Singapore, 4945-4956.

Shore Protection Manual. (1984). Coastal Engineering Research Center, Vicksburg, MS.

Tomasicchio, G.R., D'Alessandro, F., and Tundo, G. (2011). "Further developments in a new formulation of wave transmission." Proc. Coastal Structures 2011, World Scientific, Singapore, 634-645.

Vidal, C., Losada, M.A., and Mansard, E.P.D. (1995). "Stability of low-crested rubble-mound breakwater heads." J. Waterway, Port, Coastal, Ocean Eng., 121(2), 114-122.

Vidal, C., Losada, M.A., Medina, R., Mansard, E.P.D., and Gomez-Pina, G. (1992). "A universal analysis for the stability of both low-crested and submerged breakwaters." Proc. 23rd Coastal Engineering Conf., ASCE, Reston, VA, 1679-1692.

Vidal, C., and Mansard, E.P.D. (1995). "On the stability of reef breakwaters." Tech. Report, National Research Council of Canada, Ottawa, Canada.

3 PROJECT DESCRIPTION

The project site is located in the bay of Negril, Jamaica, as shown by Figure 3-1. Two low-crested breakwaters are projected in the area, as shown by Figure 3-2. Cross shore profiles for each breakwater and section details of the preliminary design provided by CEAC are shown in Figure 3-3 to Figure 3-6.

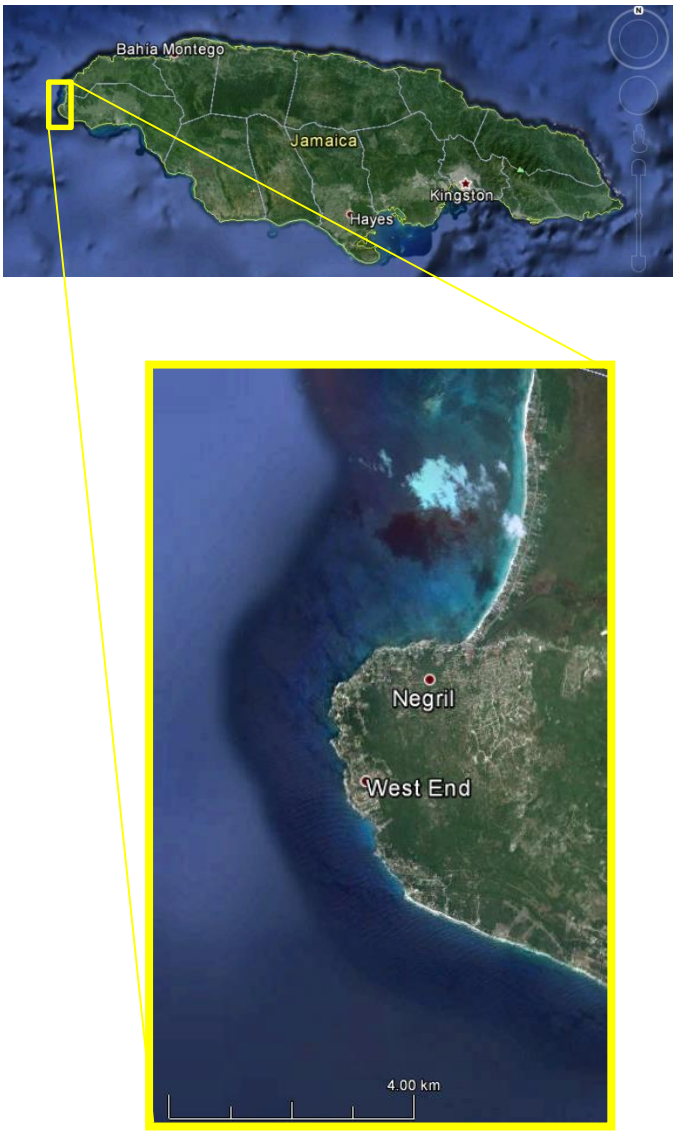

Figure 3-1: Project location.

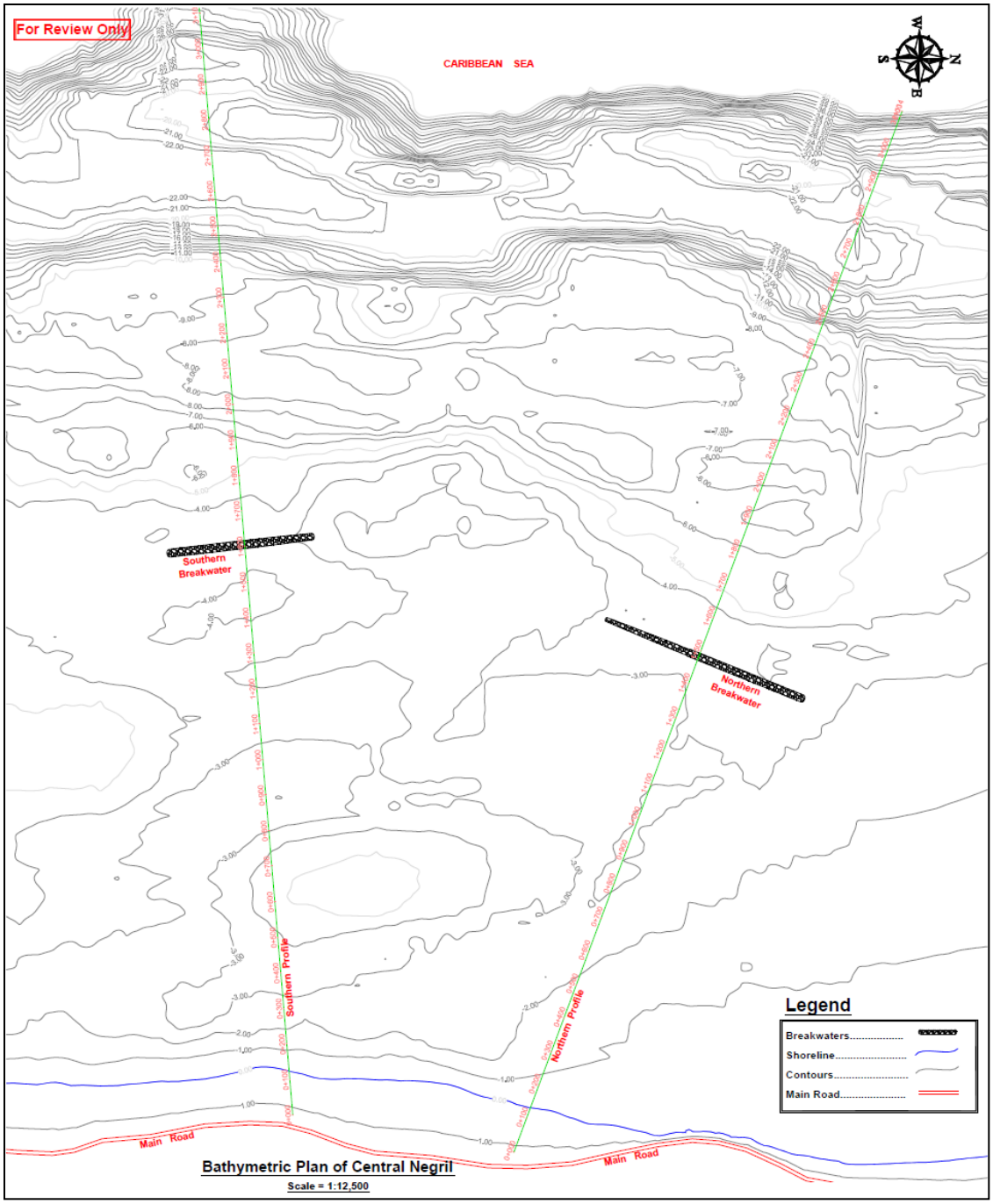

Figure 3-2: Breakwaters location.

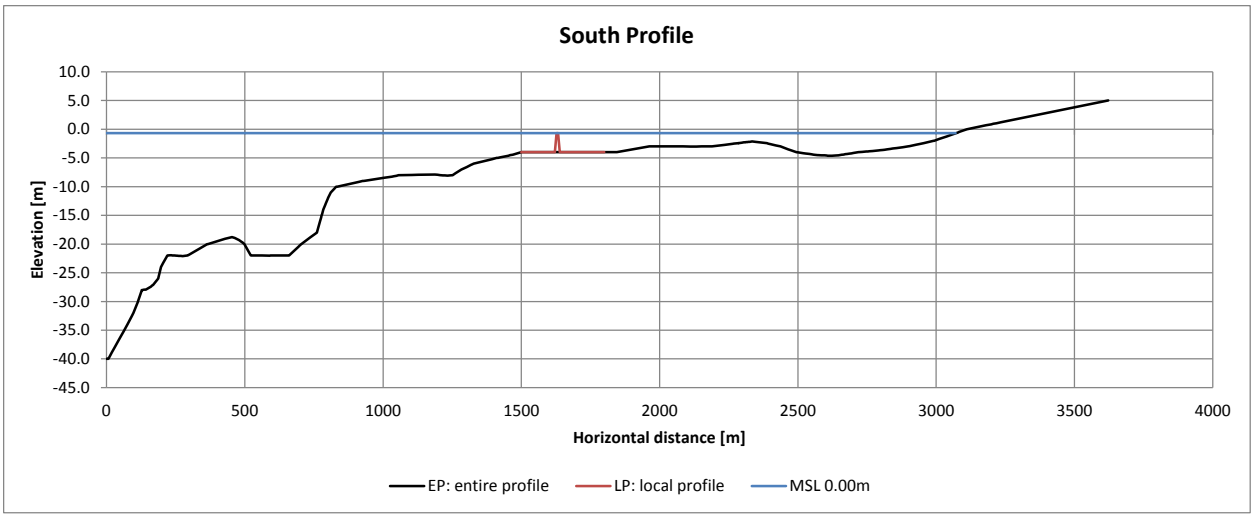

Figure 3-3: Cross-shore bathymetry profile. South breakwater.

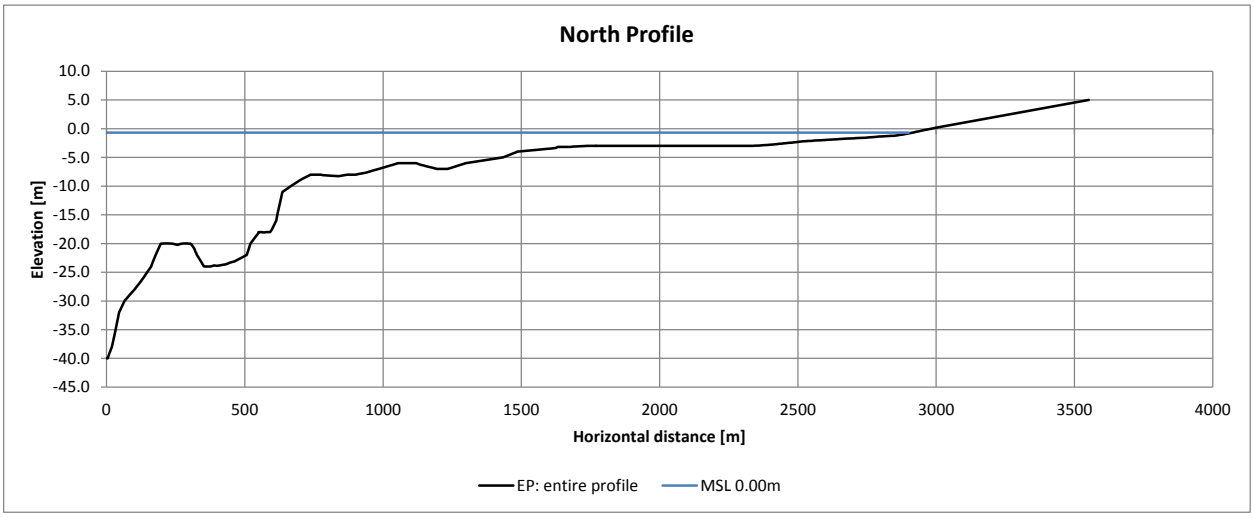

Figure 3-4: Cross-shore bathymetry profile. North breakwater.

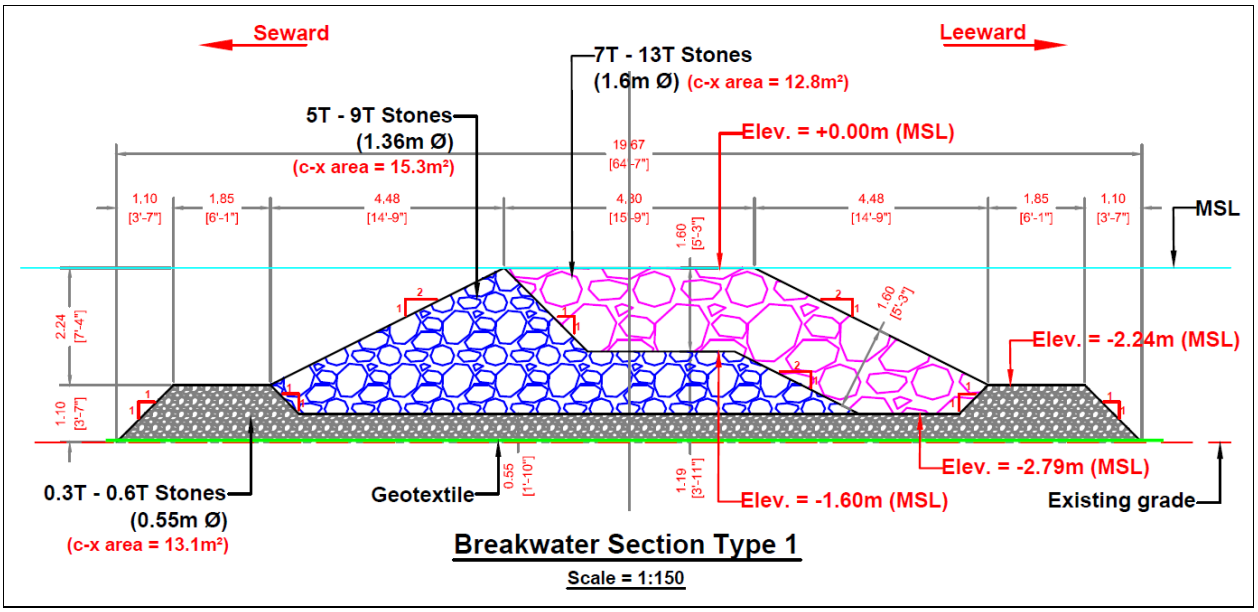

Figure 3-5: Preliminary breakwater cross-section. South Breakwater.

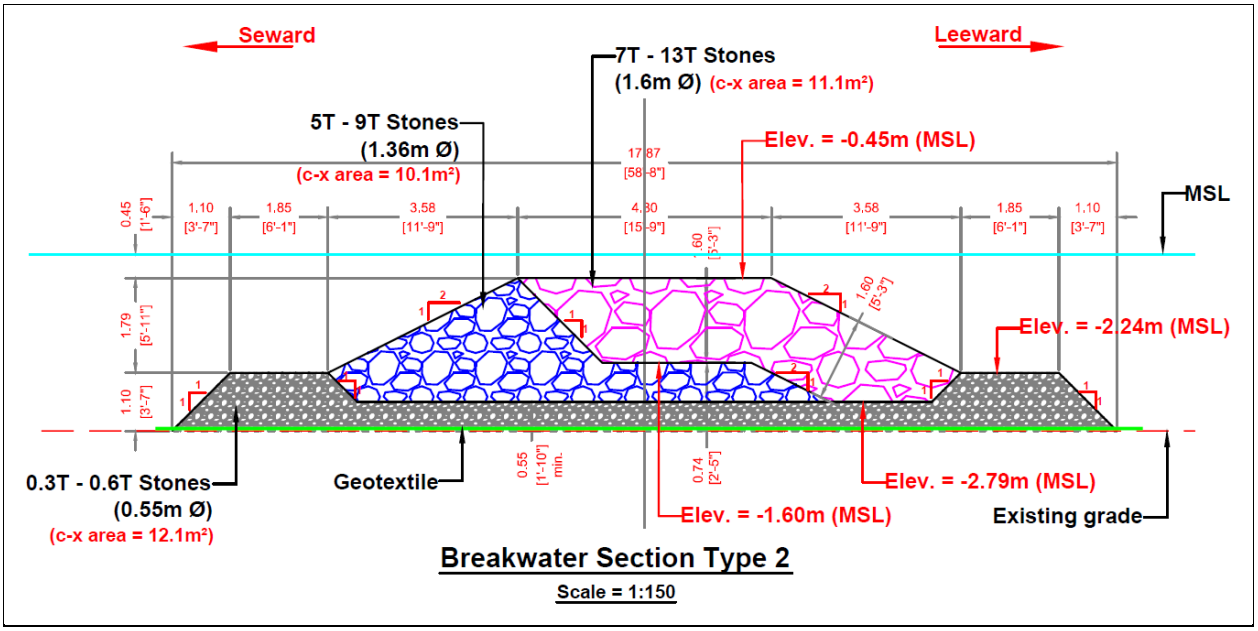

Figure 3-6: Preliminary breakwater cross-section. North Breakwater

4 NUMERICAL MODELING FOR PROTOTYPE CONDITIONS

In order to optimize testing conditions in the physical model, different scenarios were analyzed by using the "Cross-Shore Numerical Model" CSHORE, developed by CACR with support of the USACE.

Main characteristics of this numerical model are:

- Combined wave and current model based on time-averaged equations.
- Sediment transport model for suspended sand and bed load.
- Permeable layer model to account for porous flow and energy dissipation.
- Empirical formulas for irregular wave run-up and a probabilistic model for an intermittently wet and dry zone on impermeable and permeable bottoms.
- Predicting wave over-wash of a dune.
- Armor layer damage progression.

4.1 COMPUTED CASES

Computed cases were differentiated by case ID (cross-shore profile and structure conditions) and test ID (wave and water level conditions), as presented in Table 4-1 and Table 4-2.

Table 4-1: Profile and structure cases.

case ID	Profile	Structure	Armor / Toe	Gamma / Stone size	Profile	Structure	Gamma / Stone Size
case_10.00	1	0	0	0	South	no	0.70
case_10.01	1	0	0	1	South	no	0.80
case_20.00	2	0	0	0	North	no	0.70
case_11.11	1	1	1	1	South	Armor	13.0t
case_11.12	1	1	1	2	South	Armor	9.0t
case_11.13	1	1	1	3	South	Armor	7.0t
case_11.14	1	1	1	4	South	Armor	5.0t
case_11.15	1	1	1	5	South	Armor	3.0t
case_11.16	1	1	1	6	South	Armor	1.0t
case_11.21	1	1	2	1	South	Toe	0.6t
case_11.22	1	1	2	2	South	Toe	0.3t

Table 4-2: Water levels and wave conditions.

Test ID	MSL	Hs - Tp	Sea conditions MSL [m]	Hs [m]	Tp [s]
Test001	0	01	0.0	5.0	11.10
Test002	0	02	0.0	5.0	12.40
Test003	0	03	0.0	6.3	11.10
Test004	0	04	0.0	6.3	12.4
Test005	0	05	0.0	8.0	11.1
Test006	0	06	0.0	8.0	12.4
Test104	1	04	-0.5	6.3	12.4
Test106	1	06	-0.5	8.0	12.4
Test204	2	04	0.5	6.3	12.4
Test206	2	06	0.5	8.0	12.4

4.2 COMPUTED RESULTS

Results are given mainly through characterization of cross-shore wave transformation. The following figures are given in Appendix A.

- Wave transformation for the south profile for case_10.00 and tests 001 to 006, which account for changes in offshore wave height and period.
- Wave transformation for the south profile for case_10.00 and tests 104 to 206, which accounts for changes in SWL.
- Local profile near the structure in place.
- Wave transformation on the local profile for case_11.11 and tests 001 to 006.
- Wave transformation on the local profile for case_11.11 and tests 104 to 206.
- Profile damage for the armor layer of case_11.14.
- Profile damage for the toe, for case_11.21.

Computed wave transmission and structure damage were also analyzed. Results are presented bellow.

4.2.1 Wave Transmission

Wave transmission results are summarized in Figure 4-1. Use is made of an empirical formula proposed by Tomasicchio et al (2011) for comparison purposes.

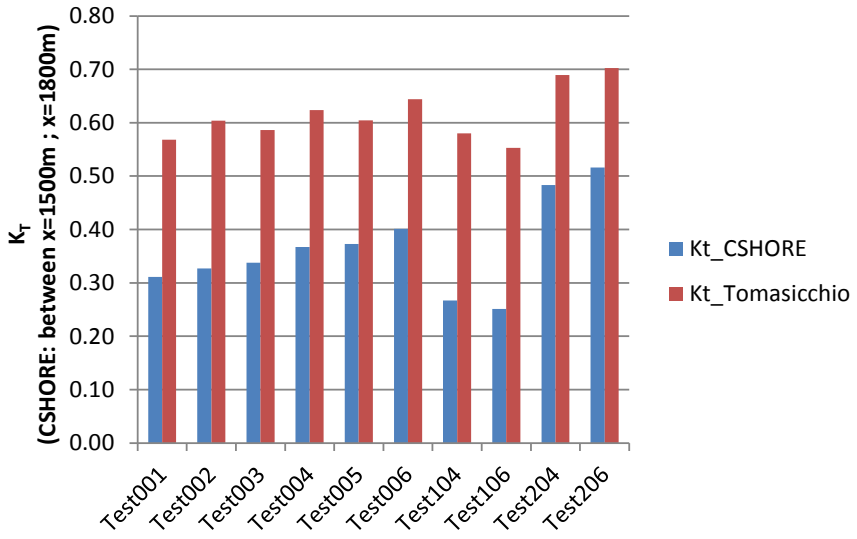

Figure 4-1: Wave transmission coefficient. Preliminary results based on numerical model and empirical formulas.

4.2.2 Structure Damage

Structure damage results are summarized in Figure 4-2. Sensitivity of stone size, which is assumed to be uniform in the numerical model for entire structure, can be verified. Similar plot is also given in Figure 4-3 for toe damage.

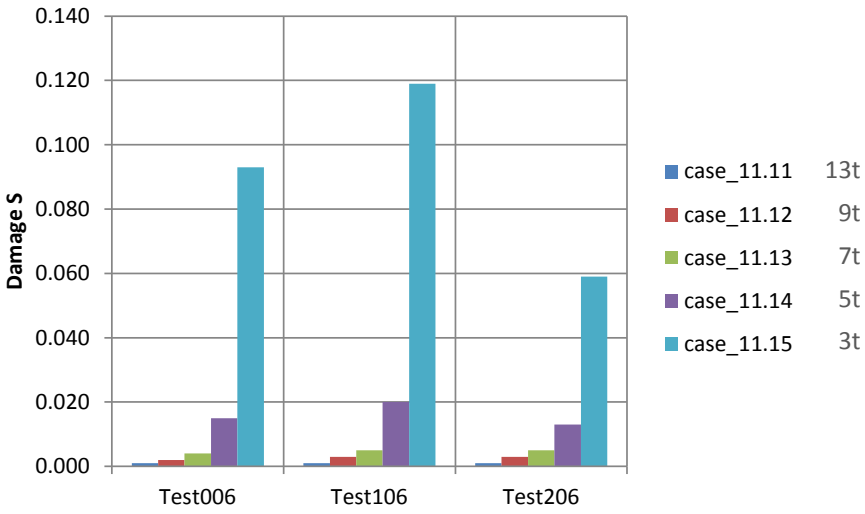

Figure 4-2: Structure damage. Preliminary results based on numerical model.

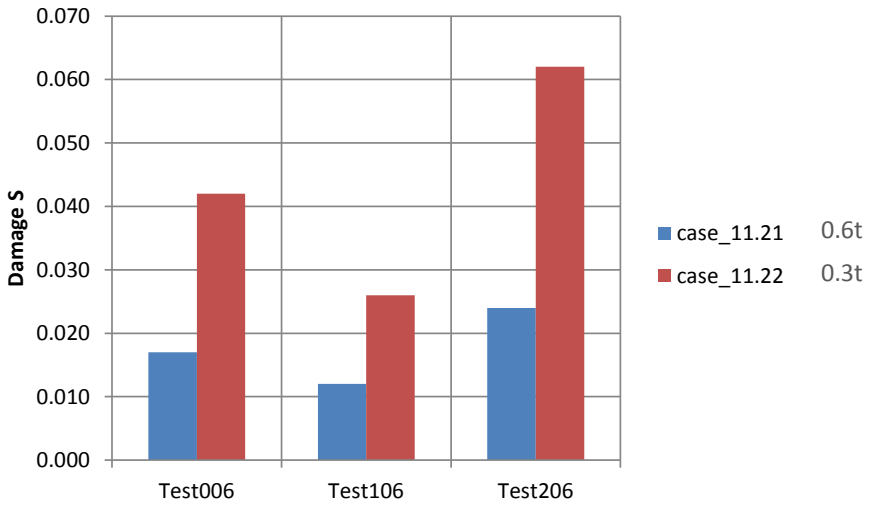

Figure 4-3: Toe damage. Preliminary results based on numerical model.

Sensitivity of wave period, wave height and water level was also verified. Results are shown in Figure 4-4, where the most consistent effect seems to be caused by water level changes, although small within the tested range.

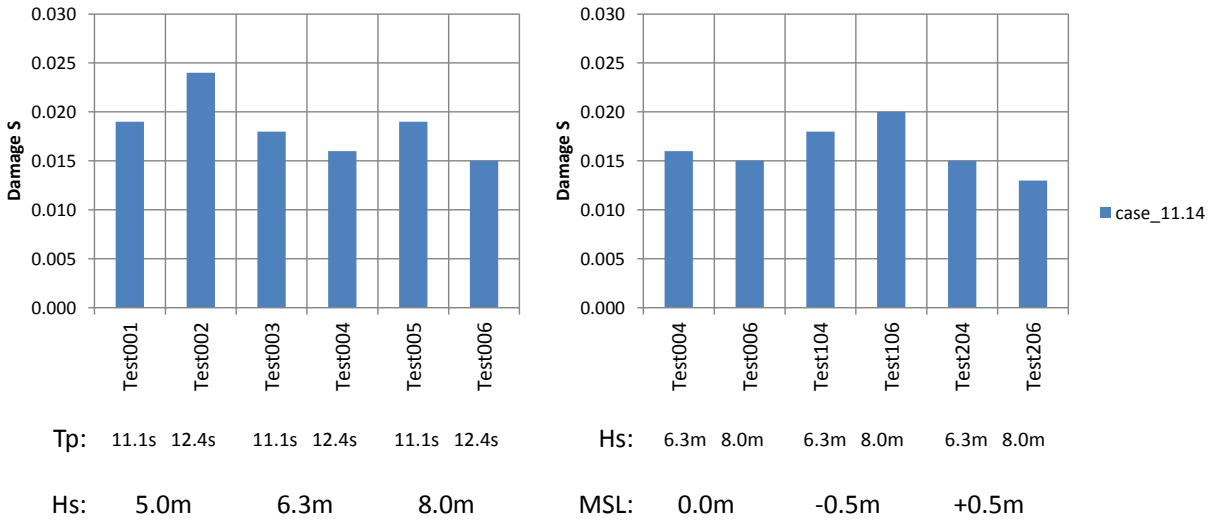

Figure 4-4: Sensitivity of damage to wave conditions. Preliminary results based on numerical model.

4.3 CONSIDERATIONS FOR PHYSICAL MODEL

Effects of wave conditions: MSL / Hs / Tp

- MSL: seems to have more consistent effect on structure stability.
- Hs: damage variations are not sensitive to offshore Hs. They may be related to differences in wave setup, since local differences in wave height are small (depth limited).
- Tp: damage variations are not sensitive to Tp.

Depth limited condition:

- For a given structure, larger water depth have counteracting effects:
  - Larger wave height.
  - Downward decrease of wave action.
- Design condition may occur frequently:
  - Damage may accumulate over years.

5 SMALL SCALE PHYSICAL MODEL

5.1 MODEL LAYOUT

Due to the similarity between both structures, only a physical model for the south breakwater was tested, since it is considered to be the most adverse case. The model was tested in a wave flume with main characteristics shown in Figure 5-1, were the water depth in front of the wavemaker was reduced to 0.8 [m] in this experiment. Wave gauges WG5 and WG6 were placed at the toe and approximately 1 [m] landward from the rear toe of the structure, respectively.

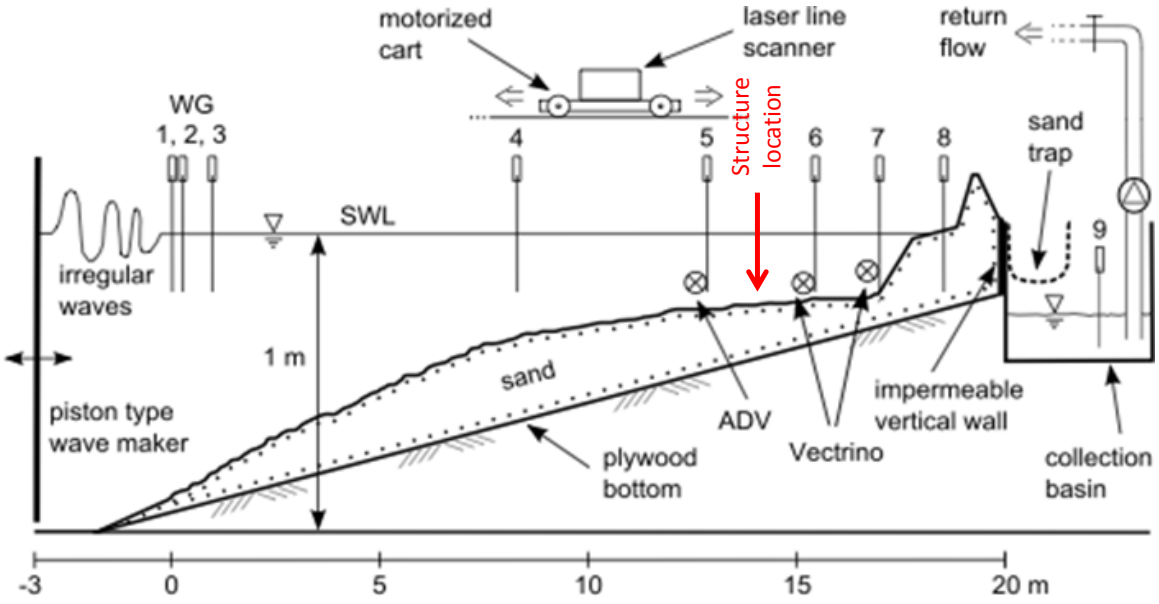

Figure 5-1: Wave flume layout.

5.2 MATERIALS

The following parameters are used to characterize stones of prototype and model:

M: stone mass [kg]

ρ_s: stone density [kg/m^3]

ρ_w: water density [kg/m^3]

D_n: nominal diameter [m]

$$\Delta = \left(\frac{\rho_s}{\rho_w} - 1\right)$$

Required stones according to preliminary prototype design are shown in Table 5-1, for which the following values have been considered:

$\rho_s = 2{,}500\ [kg/m^3]$

$\rho_w = 1{,}030\ [kg/m^3]$

Table 5-1: Prototype stones. Preliminary design given by CEAC.

Type	Δ	range of M [kg]	range of D_n [m]
Primary Armor	1.43	7,000 - 13,000	1.41 - 1.73
Secondary Armor	1.43	5,000 - 9,000	1.26 - 1.53
Base-Filter	1.43	300 - 600	0.49 - 0.62

Characteristics of the stones used in the physical model are shown in Table 5-2, for which the following value for water density has been considered:

$\rho_w = 1{,}000\ [kg/m^3]$

Table 5-2: Model stones.

Type	ρ_s [g/cm^3]	Δ	range of M (5% - 95%) [g]	range of D_n (5% - 95%) [cm]	M_{50} [g]	D_{n50} [cm]
PA01 (red)	2.65	1.65	128 - 270	3.64 - 4.67	200	4.23
SA01 (green)	2.94	1.94	102 - 158	3.26 - 3.77	128	3.52
SA02 (blue)	3.06	2.06	158 - 179	3.72 - 3.88	169	3.81
BF01 (white)	2.71	1.71	5.4 - 15.1	1.26 - 1.77	9.1	1.50

Gradation curves for each type of stone used in the physical model are shown in Figure 5-2 and Figure 5-3. For the base-filter, only BF01 type was used. Details of stones measurements are provided in Appendix B.

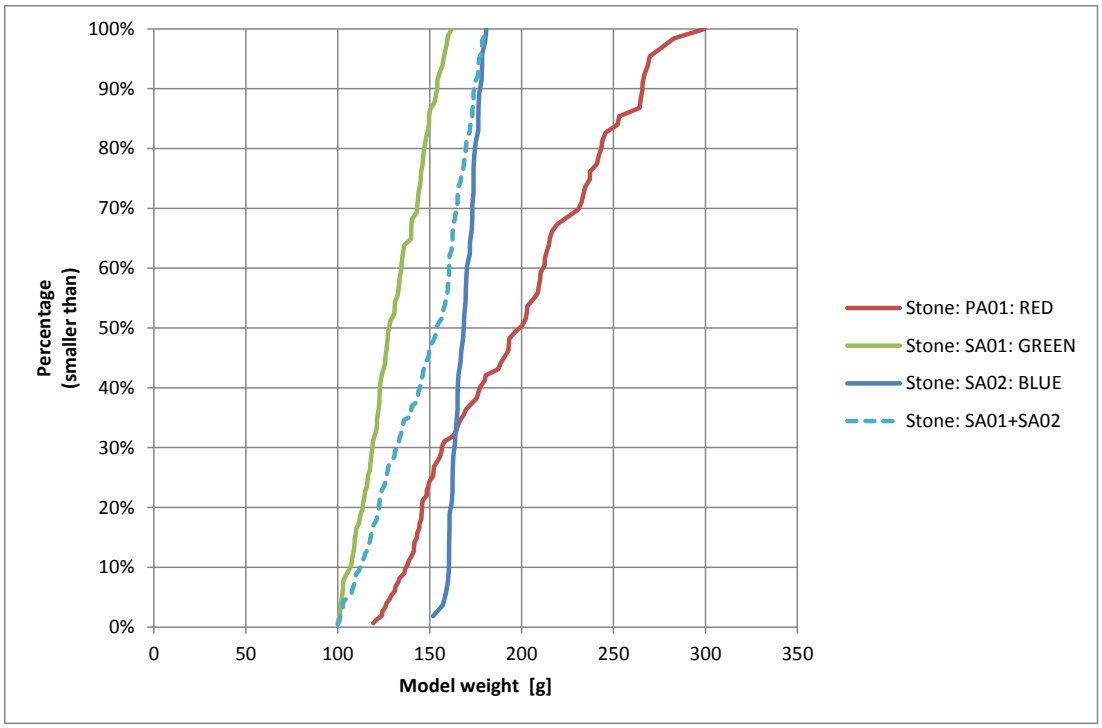

Figure 5-2: Gradation curves. Armor layer stones.

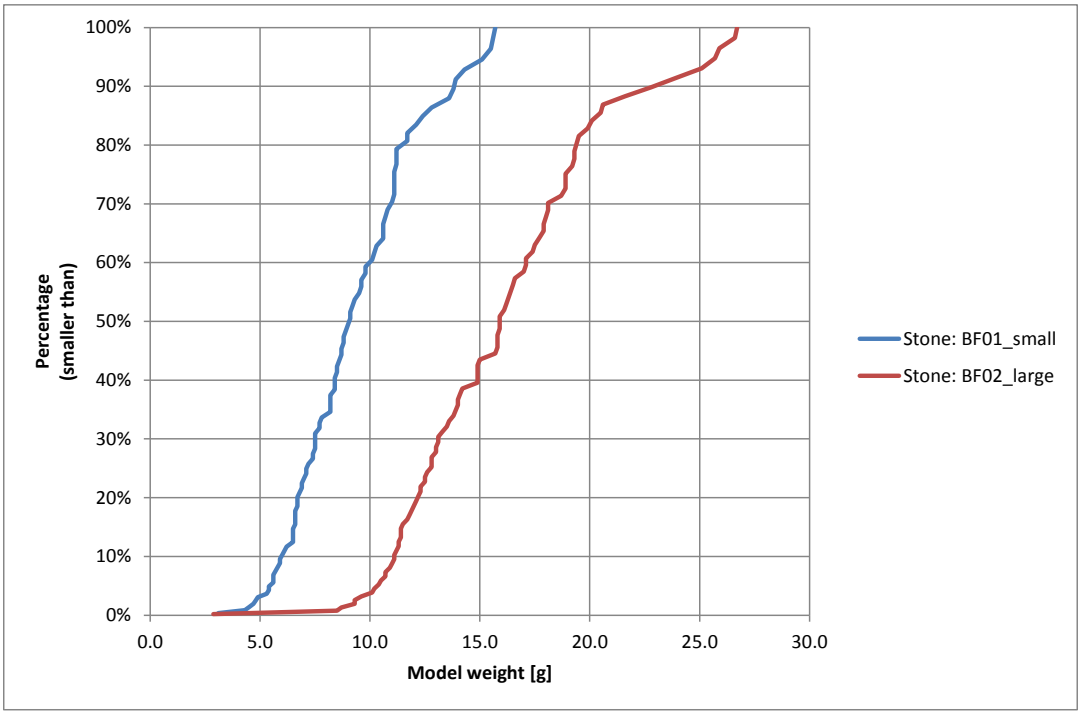

Figure 5-3: Gradation curves. Base-Filter-Toe stones.

5.3 MODEL SIMILITUDE

Model scaling is based on Froude number, which is defined as follows.

$$Fr = \frac{U}{\sqrt{g\,l}}$$: same in model and prototype.

where: U: characteristic velocity

l: characteristic length

g: acceleration of gravity (same in model and prototype)

A length scale of 1/36 was chosen between the model and the prototype, which gives a time scale of 1/6 based on Froude similitude.

Similitude between prototype and model stones may be based on Stability number Ns, which is defined as follows:

$$Ns = \frac{H_{m0}}{\Delta\, D_{n50}}$$

where: H_{m0}: spectral significant wave height at the toe of the structure

D_{n50}: nominal diameter based on median mass M_{50}, calculated as follows:

$$D_{n50} = (M_{50}/\rho_s)^{1/3}$$

According to the information provided by CEAC, the offshore wave height in the prototype is expected to be $H_{m0} \approx H_s = 6.3m$. This will produce depth limited waves at the toe of the structure. For this condition, the following relation may be assumed:

$$H_{m0} = \gamma h$$

where: γ: breaker parameter

h: water depth at the toe of the structure w/r to the still water level (SWL)

γ varies between 0.5 and 1.0, with smaller values related to gentler bottom slopes.

5.4 TEST CONDITIONS

Different structures were tested in order to improve the preliminary design. Each structure is represented by a case number. Stone composition is provided in Table 5-3. Since the sand profile in the wave flume may evolve during the experiment, two cases without the structure were tested: one at the beginning, before building any structure and one at the end, after all tests. This allows to better compare conditions with and without the breakwater. Measured profiles are shown in Appendix C.

Table 5-3: Tested cases

Case	Structure	Primary Armor	Secondary Armor	Base-Filter
case_00	No			
case_01	Yes	PA01	SA01 + SA02	BF01
case_02	Yes	SA01 + SA02		BF01
case_03	Yes	SA01		BF01
case_04	No			

Water level and wave conditions considered 2 moderate (swell) and several extreme (hurricane) wave conditions. For the latter, different water levels and wave periods were analyzed. Since depth limited wave conditions are expected at the toe of the structure, only one offshore wave height was adopted for the extreme test conditions. Table 5-4 shows the notation used to identify wave conditions in each test.

Table 5-4: Tested water levels and waves conditions

Wave period		Water level		Wave height	
T1	2.0s	D1	80cm	H1	17.5cm
T2	2.6s	D2	82cm	H2	3.9cm
T3	1.2s	D3	78cm	H3	5.0cm
T4	1.4s				

Moderate conditions were run for 6.7 [min] (1 burst) in the model, which equates 40 [min] of prototype time. In order to capture damage development under extreme conditions, a maximum of 9 bursts were run for each test. Actual tested conditions are summarized in Table 5-5.

Table 5-5: Tested conditions

Case	Test	Structure	Condition	Wave period [s]	Wave height [cm]	Water level [cm]	N° of bursts
case_00	T1D1	No	extreme	2.0	17.5	80.0	1
	T2D1	No	extreme	2.6	17.5	80.0	1
	T1D2	No	extreme	2.0	17.5	82.0	1
	T2D2	No	extreme	2.6	17.5	82.0	1
case_01	T1D1	Yes	extreme	2.0	17.5	80.0	3
	T2D1	Yes	extreme	2.6	17.5	80.0	9
	T2D2	Yes	extreme	2.6	17.5	82.0	9
case_02	T3D3	Yes	moderate	1.2	3.9	78.0	1
	T1D3	Yes	extreme	2.0	17.5	78.0	5
case_03	T3D3	Yes	moderate	1.2	3.9	78.0	1
	T4D3	Yes	moderate	1.4	5.0	78.0	1
	T1D3	Yes	extreme	2.0	17.5	78.0	6
	T1D1	Yes	extreme	2.0	17.5	80.0	3
	T1D2	Yes	extreme	2.0	17.5	82.0	3
case_04	T3D3	No	moderate	1.2	3.9	78.0	1
	T4D3	No	moderate	1.4	5.0	78.0	1
	T1D3	No	extreme	2.0	17.5	78.0	1
	T1D1	No	extreme	2.0	17.5	80.0	1
	T1D2	No	extreme	2.0	17.5	82.0	1

5.5 TEST RESULTS

Results for tested conditions are presented for each case as follows:

- **Hydrodynamic Measurements**

a) Free surface standard deviation at six wave gauge locations is presented.
   σ_η: free surface standard deviation. The following relation is used to estimate the wave height: $H_{m0} = 4\,\sigma_\eta$

The following additional information is also given for each case in Appendix D.

b) Offshore incident wave characteristics at wave gauge #1 (WG1).
   H_{m0} : spectral significant wave height
   H_{rms} : root mean square wave height
   H_s : significant wave height (average of the highest 1/3 wave heights)
   T_p : peak wave period
   T_s : significant wave period
   R : reflection coefficient

c) Mean free surface elevation at six wave gauge locations.
   $\bar{\eta}$: mean free surface elevation above the SWL of each test (wave setup)

d) Cross-shore mean and standard deviation of velocities recorded at locations of WG5 and WG6.
   $\bar{u}$: mean cross-shore velocity
   σ_u : standard deviation of cross-shore velocity (intensity of wave velocity)

- **Structure Damage**

a) Damage of the armor layer is computed using the total number of displaced stones, according to the following formulation:

$$S = \frac{N_{ox}\, D_{n50}}{(1-p)\, x}$$

   S : damage of the armor layer
   N_{ox} : number of displaced stones over the alongshore length x
   p : porosity of the armor layer (0.45)
   x : alongshore length of armor layer

The length x was defined as follows:

Case_01 and Case_02
The structure was built using the entire wave flume width $W_f = 116cm$. To disregard wall effects, the length x was defined by the following expression, considering only the nominal diameter of the combined distribution SA01+SA02 stones (green + blue).
$x = W_f - 4D_{n50}$

Case_03
The structure was built in the middle of the wave flume, using only SA01 stones. For this case, the length x was defined by discounting 1 stone diameter at each side of the structure length $W_s = 61cm$.

$x = W_s - 2D_{n50}$: for case 03 (for which the structure length was: $W_s = 61cm$)

Photographs for the initial and final conditions are provided in Appendix E.

5.5.1 Case 00: Without Breakwater (beginning)

- **Hydrodynamic Measurements**

Table 5-6: Case 00 free-surface standard deviation σ_η (cm) at six wave gauge locations.

Run	WG1	WG2	WG3	WG4	WG5	WG6
T1D1_1	4.48	4.48	4.48	4.39	2.33	1.70
T1D2_1	4.40	4.40	4.37	4.20	2.56	1.82
T2D1_1	4.61	4.57	4.60	4.64	2.43	1.83
T2D2_1	4.48	4.49	4.48	4.48	2.79	2.01

5.5.2 Case 01: With Breakwater (PA01+SA01+SA02)

- **Hydrodynamic Measurements**

Table 5-7: Case 01 (T1D1) free-surface standard deviation σ_η (cm) at six wave gauge locations.

Run	WG1	WG2	WG3	WG4	WG5	WG6
T1D1_1	4.20	4.15	4.25	4.24	NR	NR
T1D1_2	4.22	4.17	4.26	4.26	NR	NR
T1D1_3	4.25	4.20	4.28	4.27	NR	NR

NR implies "not reliable" data

Table 5-8: Case 01 (T2D1) free-surface standard deviation σ_η (cm) at six wave gauge locations.

Run	WG1	WG2	WG3	WG4	WG5	WG6
T2D1_1	4.22	4.19	4.27	4.31	2.55	1.36
T2D1_2	4.25	4.21	4.31	4.33	2.55	1.36
T2D1_3	4.26	4.24	4.32	4.35	2.56	1.35
T2D1_4	4.27	4.25	4.34	4.36	2.59	1.37
T2D1_5	4.28	4.26	4.33	4.37	2.59	1.36
T2D1_6	4.28	4.27	4.32	4.35	2.58	1.37
T2D1_7	4.25	4.24	4.30	4.38	2.59	1.37
T2D1_8	4.25	4.25	4.31	4.37	2.59	1.38
T2D1_9	4.26	4.24	4.31	4.37	2.60	1.38

Table 5-9: Case 01 (T2D2) free-surface standard deviation σ_η (cm) at six wave gauge locations.

Run	WG1	WG2	WG3	WG4	WG5	WG6
T2D2_1	4.13	4.15	4.20	4.29	2.95	1.63
T2D2_2	4.16	4.18	4.24	4.30	2.97	1.64
T2D2_3	4.18	4.21	4.27	4.32	2.97	1.65
T2D2_4	4.20	4.23	4.28	4.32	2.95	1.65
T2D2_5	4.20	4.23	4.30	4.33	2.97	1.66
T2D2_6	4.18	4.23	4.27	4.30	2.98	1.64
T2D2_7	4.18	4.22	4.28	4.30	3.00	1.64
T2D2_8	4.17	4.20	4.27	4.29	2.99	1.64
T2D2_9	4.18	4.20	4.27	4.29	3.00	1.65

- **Structure Damage**

The structure was repaired after the last burst of each extreme test condition T1D1, T2D1 and T2D2. Damage results are shown in Table 5-10.

Table 5-10: Case 01 armor damage.

Parameter	Tests		
	T1D1	T2D1	T2D2
N_{ow}	0	3	1
D_{n50} [cm]	3.7	3.7	3.7
x [cm]	101	101	101
p	0.45	0.45	0.45
Damage S	**0.0**	**0.2**	**0.1**

5.5.3 Case 02: With Breakwater (SA01+SA02)

- **Hydrodynamic Measurements**

Table 5-11: Case 02 free-surface standard deviation σ_η (cm) at six wave gauge locations.

Run	WG1	WG2	WG3	WG4	WG5	WG6
T3D3_1	1.05	1.11	1.03	0.97	NR	NR
T1D3_1	4.31	4.13	4.35	4.38	NR	NR
T1D3_2	4.34	4.15	4.38	4.40	NR	NR
T1D3_3	4.35	4.18	4.39	4.42	NR	NR
T1D3_4	4.37	4.16	4.41	4.42	NR	NR
T1D3_5	4.37	4.18	4.42	4.42	NR	NR

NR implies "not reliable" data

- **Structure Damage**

Table 5-12: Case 02 armor damage.

Parameter	Tests T1D3
N_{ow}	3
D_{n50} [cm]	3.7
x [cm]	101
p	0.45
Damage S	**0.2**

5.5.4 Case 03: With Breakwater (SA01)

- **Hydrodynamic Measurements**

Table 5-13: Case 03 free-surface standard deviation σ_η (cm) at six wave gauge locations.

Run	WG1	WG2	WG3	WG4	WG5	WG6
T3D3_1	1.00	0.98	1.00	0.91	0.81	0.48
T4D3_1	1.30	1.28	1.30	1.23	1.06	0.62
T1D3_1	4.19	4.14	4.26	4.25	2.39	1.32
T1D3_2	4.20	4.17	4.29	4.25	2.40	1.32
T1D3_3	4.23	4.19	4.31	4.27	2.43	1.35
T1D3_4	4.23	4.21	4.31	4.28	2.42	1.35
T1D3_5	4.22	4.19	4.31	4.27	2.43	1.35
T1D3_6	4.21	4.19	4.31	4.28	2.44	1.35
T1D1_1	4.19	4.21	4.26	4.23	2.63	1.53
T1D1_2	4.20	4.23	4.27	4.23	2.63	1.54
T1D1_3	4.21	4.23	4.27	4.23	2.64	1.56
T1D2_1	4.05	4.02	4.06	3.91	2.78	1.73
T1D2_2	4.04	4.00	4.06	3.92	2.79	1.74
T1D2_3	4.06	4.03	4.07	3.93	2.79	1.74

- **Structure Damage**

Table 5-14: Case 03 armor damage.

Parameter	Tests T1D3+T1D1+T1D2
N_{ow}	6
D_{n50} [cm]	3.5
x [cm]	54
p	0.45
Damage S	**0.7**

5.5.5 Case 04: Without Breakwater (end)

- **Hydrodynamic Measurements**

Table 5-15: Case 04 free-surface standard deviation σ_η (cm) at six wave gauge locations.

Run	WG1	WG2	WG3	WG4	WG5	WG6
T3D3_1	0.97	0.96	0.93	0.89	0.91	0.92
T4D3_1	1.27	1.28	1.25	1.21	1.25	1.11
T1D3_1	4.24	4.24	4.26	4.24	2.47	1.65
T1D1_1	4.29	4.29	4.30	4.25	2.72	1.94
T1D2_1	4.07	4.06	4.10	3.98	2.84	2.22

5.6 DATA ANALYSIS

The results for the optimized structure of case 03 were analyzed in order to better characterize the wave transmission and structure damage.

5.6.1 Wave Transmission

Since the water depth at the location of WG5 (at the toe of the structure) is different from the one at WG6 (approximately 1 [m] landward from the rear toe of the structure), wave transformation needs be considered.

Effects of wave transformation between WG5 and WG6, without the structure, are given in Table 5-16 based on the results of case 04. Wave transformation and transmission with the structure are shown in Table 5-17, based on the results of case 03. The following three parameters are computed for each test condition:

- $T = \frac{H_{m0\ at\ WG6}}{H_{m0\ at\ WG5}}$;
- $T' = \frac{H_{m0\ at\ WG6\ with\ structure}}{H_{m0\ at\ WG6\ without\ structure}}$;
- $\gamma = \frac{H_{m0\ at\ WG5}}{depth\ at\ WG5\ (toe)}$;

Table 5-16: Wave transformation and transmission between WG5 and WG6. Case_04.

Run	SWL (cm)	Toe Elevation (cm)	Water Depth at Toe (cm)	Without Structure			γ (at WG5)
				WG5 H_{m0} (cm)	WG6 H_{m0} (cm)	T	
T3D3_1	78	66	12	3.64	3.68	1.01	
T4D3_1	78	66	12	5.00	4.44	0.89	
T1D3_1	78	66	12	9.88	6.60	0.67	0.82
T1D1_1	80	66	14	10.88	7.76	0.71	0.78
T1D2_1	82	66	16	11.36	8.88	0.78	0.71

Table 5-17: Wave transformation and transmission between WG5 and WG6. Case_03.

Run	SWL (cm)	Toe Elevation (cm)	Water Depth at Toe (cm)	With Structure			T' (WG6) With/Without	γ (at WG5)
				WG5 H_{m0} (cm)	WG6 H_{m0} (cm)	T		
T3D3_1	78	66	12	3.24	1.92	0.59	0.52	
T4D3_1	78	66	12	4.24	2.48	0.58	0.56	
T1D3_1	78	66	12	9.56	5.28	0.55	0.80	0.80
T1D3_2	78	66	12	9.60	5.28	0.55	0.80	0.80
T1D3_3	78	66	12	9.72	5.40	0.56	0.82	0.81
T1D3_4	78	66	12	9.68	5.40	0.56	0.82	0.81
T1D3_5	78	66	12	9.72	5.40	0.56	0.82	0.81
T1D3_6	78	66	12	9.76	5.40	0.55	0.82	0.81
T1D1_1	80	66	14	10.52	6.12	0.58	0.79	0.75
T1D1_2	80	66	14	10.52	6.16	0.59	0.79	0.75
T1D1_3	80	66	14	10.56	6.24	0.59	0.80	0.75
T1D2_1	82	66	16	11.12	6.92	0.62	0.78	0.70
T1D2_2	82	66	16	11.16	6.96	0.62	0.78	0.70
T1D2_3	82	66	16	11.16	6.96	0.62	0.78	0.70

5.6.2 Structure Damage

Damage development of the armor layer during test conditions of case 03 is shown in Figure 5-4. It can be seen that most of the stones were displaced at the beginning of the first extreme condition (T1D3). Afterwards damage progression was reduced and no major changes in damage trend were observed due to the increase of the water level.

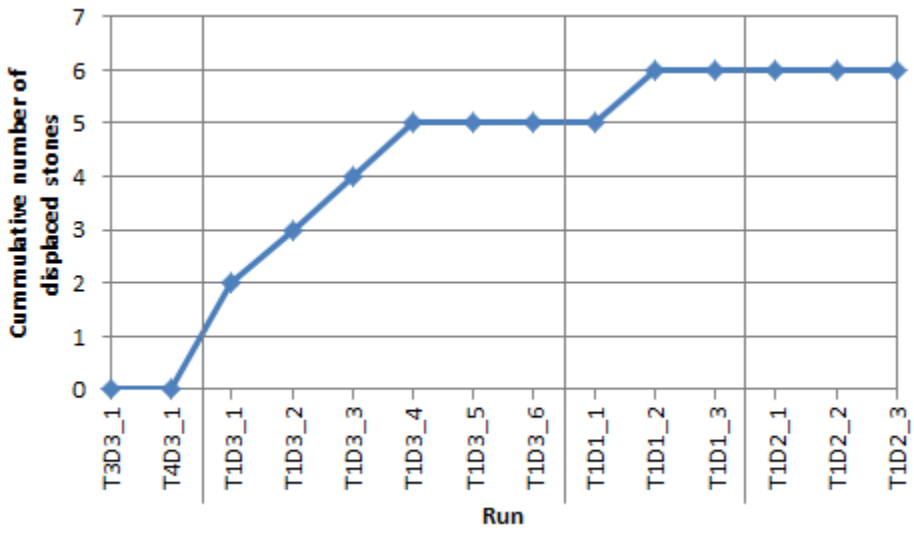

Figure 5-4: Damage development. Case_03.

All structures tested in the physical model considered the use of stones BF01 (Table 5-2) for the base/toe of the breakwater. Spreading of the toe was verified in all tests, particularly in the front side. Nevertheless, stone size and toe volume were enough to provide support for the armor layer.

Stability number Ns (defined in section §5.3) for the stones of the armor layer and toe, for each run of case 03, is shown in Table 5-18

Table 5-18: Stability numbers

Run	Water Depth at Toe (cm)	WG5 T_p (s)	WG5 H_{m0} (cm)	Ns (armor)	Ns (toe)
T3D3_1	12	1.2	3.24	-	-
T4D3_1	12	1.4	4.24	-	-
T1D3_1	12	2.0	9.56	1.40	3.73
T1D3_2	12	2.0	9.60	1.41	3.74
T1D3_3	12	2.0	9.72	1.42	3.79
T1D3_4	12	2.0	9.68	1.42	3.77
T1D3_5	12	2.0	9.72	1.42	3.79
T1D3_6	12	2.0	9.76	1.43	3.81
T1D1_1	14	2.0	10.52	1.54	4.10
T1D1_2	14	2.0	10.52	1.54	4.10
T1D1_3	14	2.0	10.56	1.55	4.12
T1D2_1	16	2.0	11.12	1.63	4.34
T1D2_2	16	2.0	11.16	1.63	4.35
T1D2_3	16	2.0	11.16	1.63	4.35

For the first extreme condition T1D3, where most of the stone displacement occurred, stability number is approximately $Ns = 1.4$ for the stones of the armor layer; and $Ns = 3.7$ for the stones of the toe. In order to limit the damage of the prototype to the conditions observed in the physical model, the stability number of the prototype should not exceed these values.

6 ASSESMENT OF DESIGN RECOMMENDATION

Based on results and observations of the physical model, the following simplification and adjustments are proposed, followed by a final verification based on empirical formulas and numerical modelling.

6.1 DESIGN RECOMMENDATION

The required prototype stone size is calculated by:

$$D_{n50} = \frac{H_{m0}}{\Delta\, Ns} = \frac{\gamma h}{\Delta\, Ns}$$

$$M_{50} = \rho_s\, {D_{n50}}^3$$

Considering the information of the available stones for the prototype (Table 5-1) and the following values for design parameters, the required stone size is given in Table 6-1.

- $(Ns)_{armor} = 1.2$; reduced from 1.4 obtained from the physical model.
- $(Ns)_{toe} = 3.2$; reduced from 3.7 obtained from the physical model.
- $\gamma = 0.6$; breaker parameter on true gentle beach slope at the project site.
- $h = 4m$; approximate water depth for minimum stability on low-crested structure (structure slightly submerged).

Table 6-1: Required stone size for prototype

Parameter		Armor	Toe
Ns		1.20	3.20
ρ_s	[kg/m^3]	2500	2500
ρ_w	[kg/m^3]	1030	1030
Δ		1.43	1.43
h	[m]	4.00	4.00
γ		0.60	0.60
H_{m0}	[m]	2.40	2.40
D_{n50}	[m]	1.40	0.53
M_{50}	[t]	6.9	0.4

According to recommendation of the Shore Protection Manual (SPM), the range of stone size for the armor layer can be specified as:

M_{armor}: $0.75\,M_{50}$ $-$ $1.25\,M_{50}$

The stone size and range of the toe and underlayer can be specified on the basis of armor layer stone size as:

$M_{toe} = \frac{M_{armor}}{10}$

The SPM guideline gives more conservative result for the toe and could help reducing stone movement seen during the experiment.

Finally, the recommended stone size and range for the prototype is given in Table 6-2.

Table 6-2: Recommended stone size for prototype

Parameter		Armor	Toe
M_{50}	[t]	7	0.7
range	[t]	5 – 9 (or larger)	0.5 – 0.9 (or larger)

6.2 EMPIRICAL FORMULAS

The following input data is specified:

DATA			
Incident wave conditions			
d_{SWL}	3.34	m	*water depth at the toe of the structure (w/r to SWL)*
η_{SWL}	0.00	m	*water surface elevation (w/r to SWL)*
h	3.34	m	*water depth at the toe of the structure*
H_{m0}	6.30	m	*preliminary incident wave height*
T_p	12.4	s	*peak wave period*
L_0	240.1	m	*deepwater wavelength*
L	69.9	m	*local wavelength*
tan(β)	0.02		*foreshore slope (V:H)*
ξ	0.12		*foreshore surf similarity parameter*
γ_e	0.60		*approximate breaker parameter*
spilling breaker			*breaker type*
depth-limited			*checking for depth-limited waves*
γ	0.60		*breaker parameter to be used*
H_{m0}	2.00	m	*incident wave height at the toe of the structure to be used*

Structure characteristics			
ρ_w	1030	kg/m^3	*water density*
ρ_r	2500	kg/m^4	*stone density*
Δ	1.43		*relative density*
tan(α)	0.50		*structure slope (V:H)*
B	5.00	m	*structure's crest width*
h_c	3.34	m	*structure height*
R_c	0.00	m	*crest freeboard (positive upward)*
Low-crested breakwater			

6.2.1 Wave Transmission

Use is made of formulation proposed by Tomasicchio et al (2011) to calculate wave transmission. For a water depth at the crest of the structure, the transmission coefficient over and through the structure is 0.56.

H_i	2.00	m	*incident wave height at the toe of the structure*
D_{eff}	1.41	m	*effective diameter (D_{n50}) Impermeable structures D_{eff}=0*
B_{eff}	6.34	m	*effective width of the structure*
a	1.00		
$R_{c,0}$	0.80		
C	9.2		
K_h	0.63		
K_{t_over}	0.55		*transmitted wave coeff over the structure*
K_{t_thru}	0.15		*transmitted wave coeff through the structure*
K_{t_all}	0.56		*transmitted wave coeff*
H_t	1.12	m	*transmitted wave height at the rear toe of the structure*

6.2.2 Structure Damage

Use is made of the formulation proposed by Kramer and Burcharth (2003) to calculate the required stone of the armor layer for a low-crested structure subjected to depth limited breaking waves.

Formulations

$$\frac{H_s}{\Delta D_{n50}} = a\left(\frac{R_c}{D_{n50}}\right)^2 - b\left(\frac{R_c}{D_{n50}}\right) + c$$

$$H_s = \gamma h;\ \gamma' = \gamma/\Delta$$

$$u = \frac{R_c}{h_c};\ v = \frac{D_{n50}}{h_c};\ -3 \le \frac{u}{v} < 2$$

$$u_* = \frac{(\gamma' - b)}{4ac}\left\{[(\gamma' - b)u_* - \gamma'] - \sqrt{[(\gamma' - b)u_* - \gamma']^2 - 4ac\ {u_*}^2}\right\}$$

$$v = \frac{1}{2c}\left\{\sqrt{[(\gamma' - b)u - \gamma']^2 - 4ac\ u^2} - [(\gamma' - b)u - \gamma']\right\}$$

Results			
γ'	0.42		*γ' = γ/Δ*
curve	curve 0		*Kramer and Burcharth (2003)*
a	0.06		*Kramer and Burcharth (2003)*
b	0.23		*Kramer and Burcharth (2003)*
c	1.36		*Kramer and Burcharth (2003)*
u_*	-0.55		*Rc/Hc*
v_{max}	0.35		*Dn50/Hc*
u/v	-1.59	ok!	
D_{n50}	**1.16**	**m**	*required stone size*
W_{50}	**3.9**	**t**	*required stone weight*

This empirical formula predicts $M_{50} = 3.9\,[t]$, but has never been verified for a low-crested structure located well inside the surf zone, corresponding to the condition of Negril breakwater during severe storms.

6.3 NUMERICAL MODEL

The Cross-Shore Numerical Model (CSHORE) is used to verify the recommended design. The following input conditions have been specified:

CSHORE INPUT DATA			
Incident wave conditions			
d_{SWL}	3.34	m	*water depth at the toe of the structure (w/r to SWL)*
η_{SWL}	0.66	m	*water surface elevation (w/r to SWL)*
h	4.00	m	*water depth at the toe of the structure*
H_{m0}	6.30	m	*preliminary incident wave height*
T_p	12.4	s	*peak wave period*
time	12	hr	*simulation time*
Structure characteristics			
ρ_w	1030	kg/m^3	*water density*
ρ_r	2500	kg/m^4	*stone density*
Δ	1.43		*relative density*
Stability of armor layer			
W_{50}	7.0	t	*specified stone weight*
D_{n50}	1.41	m	*specified stone diamter*
Stability of toe			
W_{50}	0.7	t	*specified stone weight*
D_{n50}	0.65	m	*specified stone diamter*

6.3.1 Wave Transmission

The computed wave transmission coefficient for the specified conditions is 0.4. Wave transformation over the structure is detailed in the figures of Appendix F.

The transmission coefficient calculated with CSHORE is smaller than 0.56 in section §6.2.1 using Tomasicchio et al (2011).

6.3.2 Structure Damage

Structure damage is verified with CSHORE. Damage evolution during a storm duration of 12hr was computed. Results are shown in Figure 6-1.

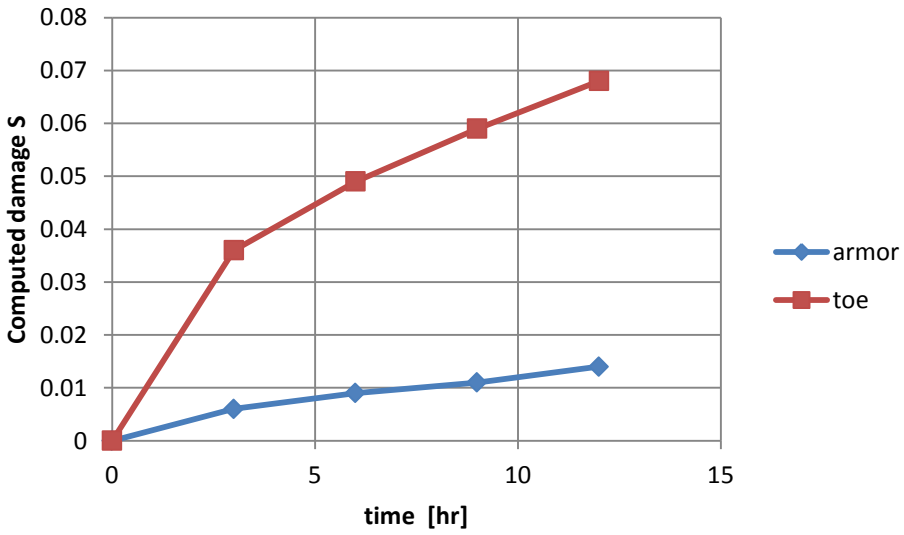

Figure 6-1: Computed damage evolution.

It can be verified that despite the increase of damage with time, calculated values are much smaller than damage S=1, for both armor layer and toe, where S=1 is normally regarded as the initiation of damage.

Results of eroded profiles for the armor layer and toe are given in Appendix F.

APPENDIX A

Results of numerical model for

specification of testing conditions in physical model

Wave transformation for the south profile. Case_10.00 – Tests 001 – 006

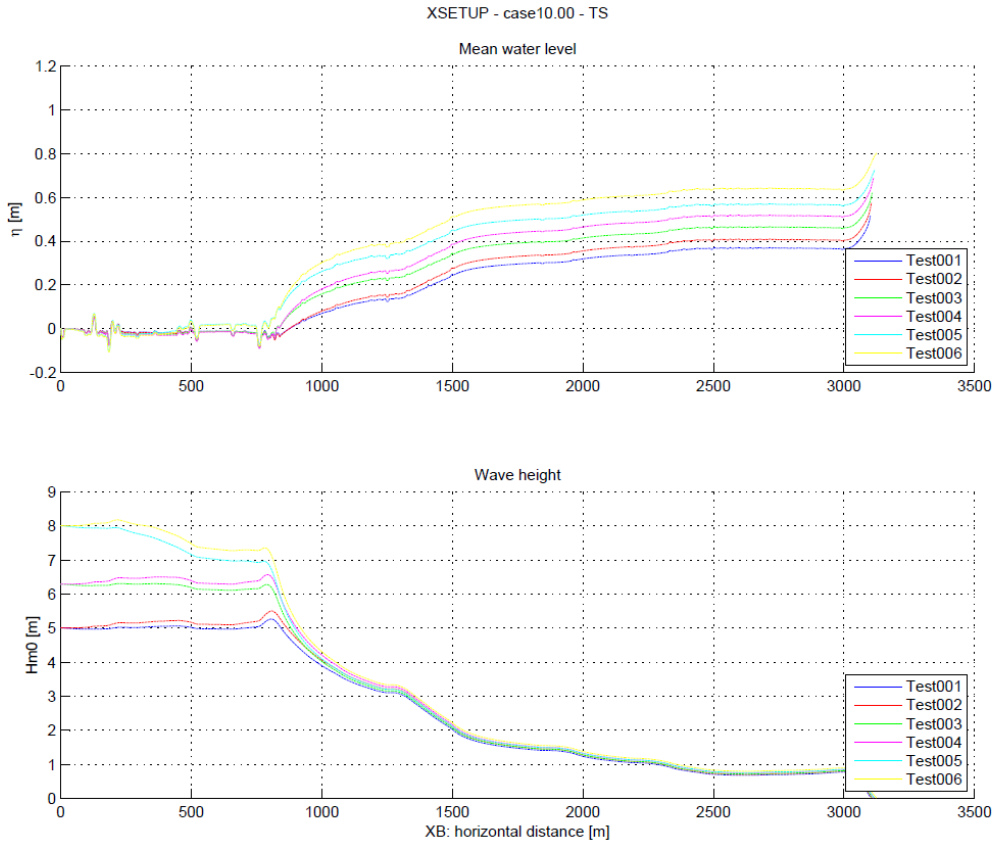

Wave transformation for the south profile. Case_10.00 – Tests 104 – 206

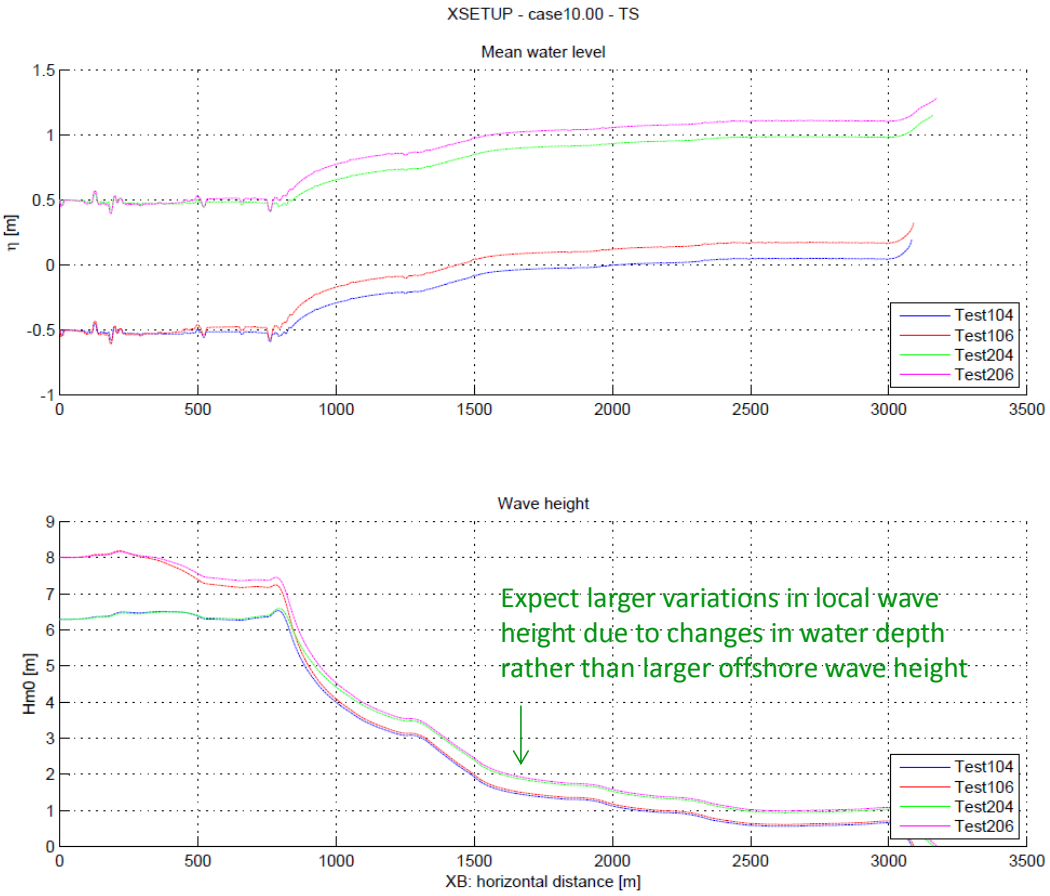

Local profile

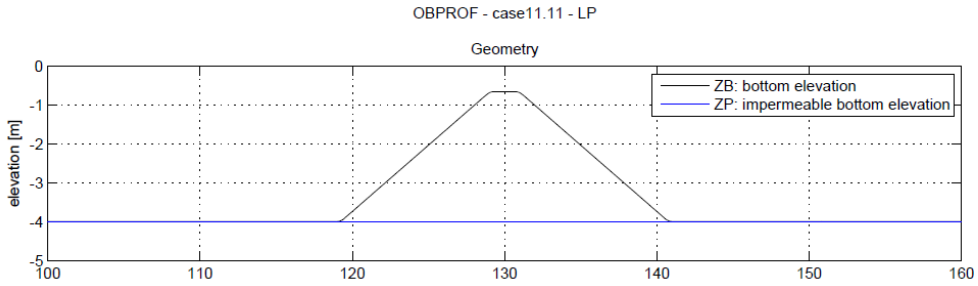

Wave transformation on the local profile. Case_11.11 - tests 001 to 006.

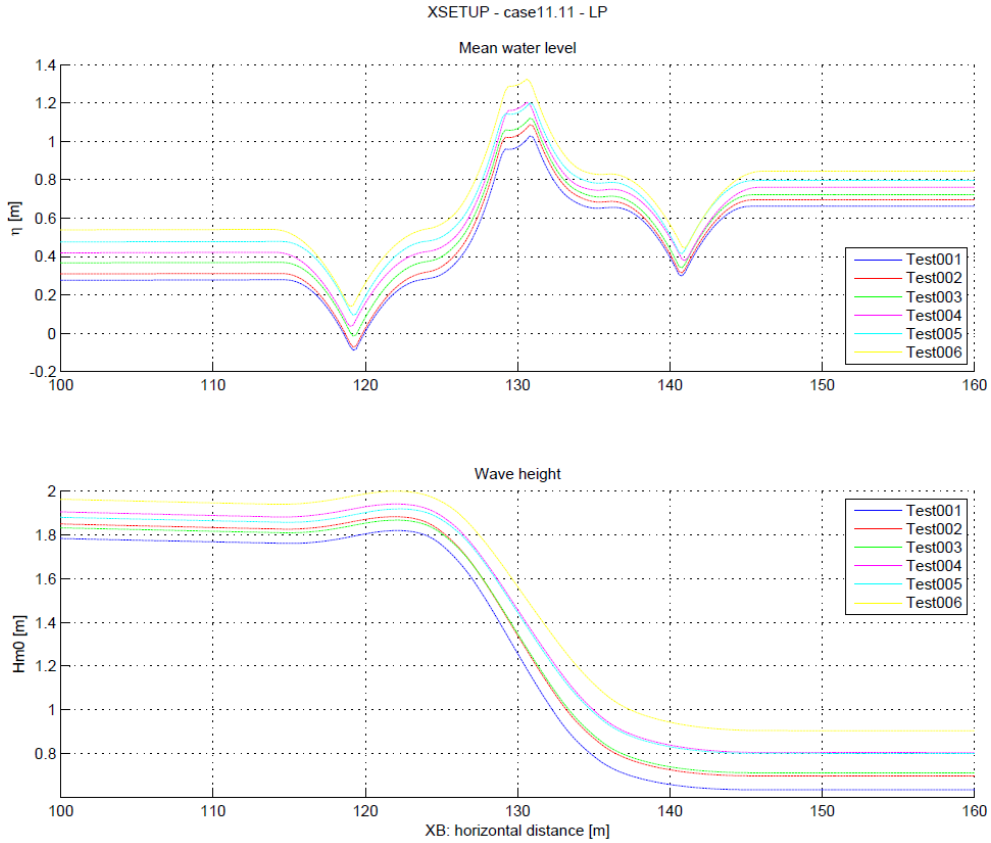

Wave transformation on the local profile. Case_11.11 - tests 104 to 206.

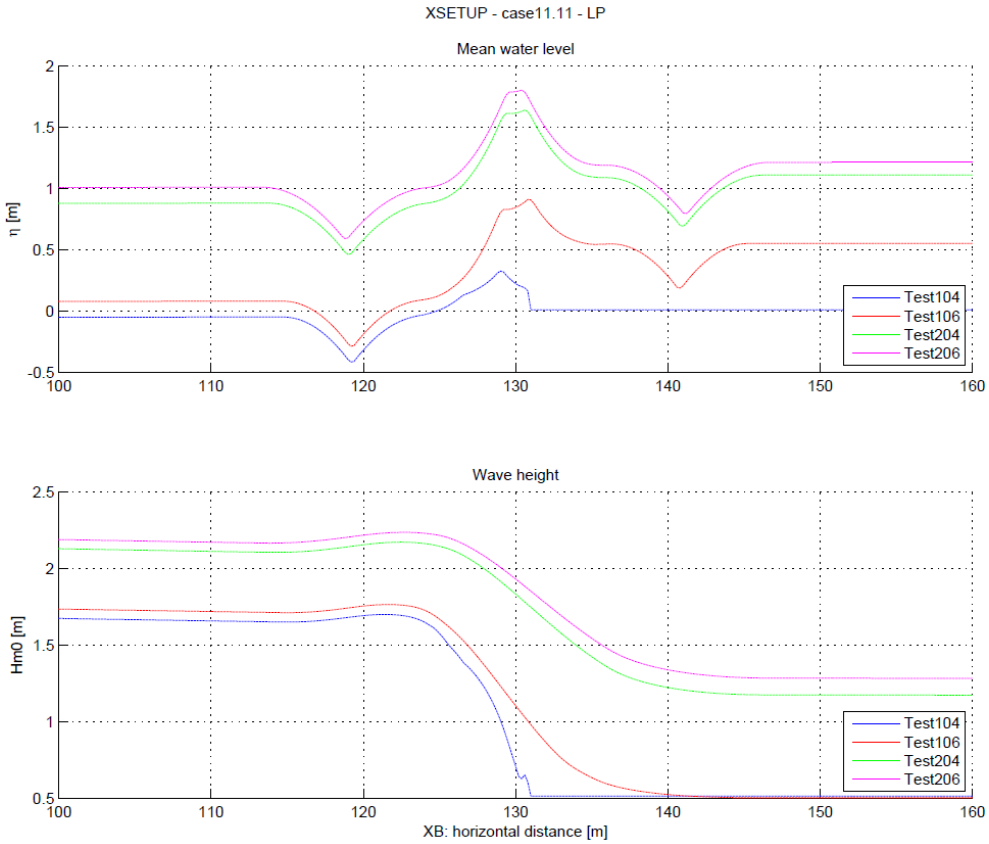

Profile damage for the armor layer. Case_11.14.

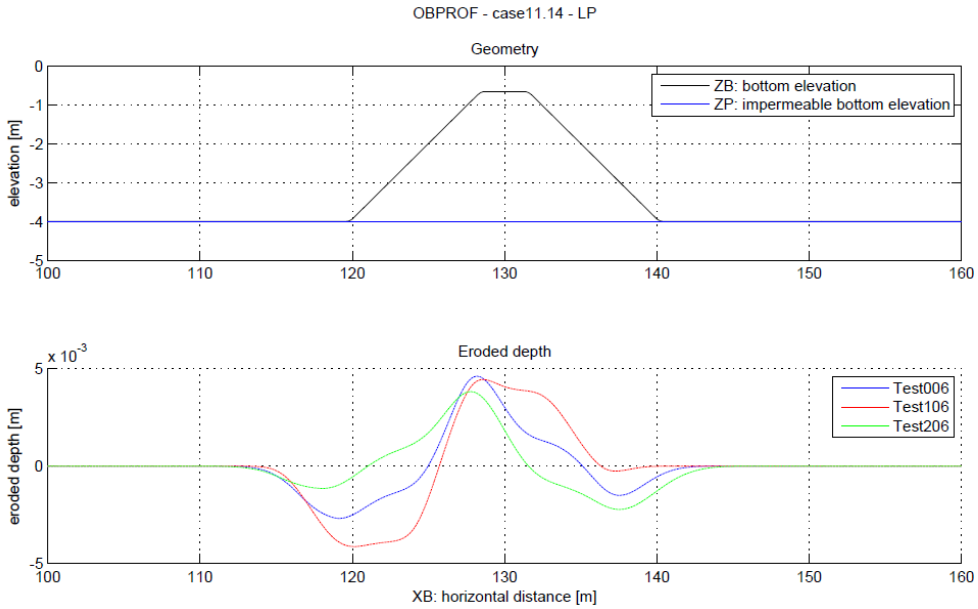

Profile damage for the toe. Case_11.21.

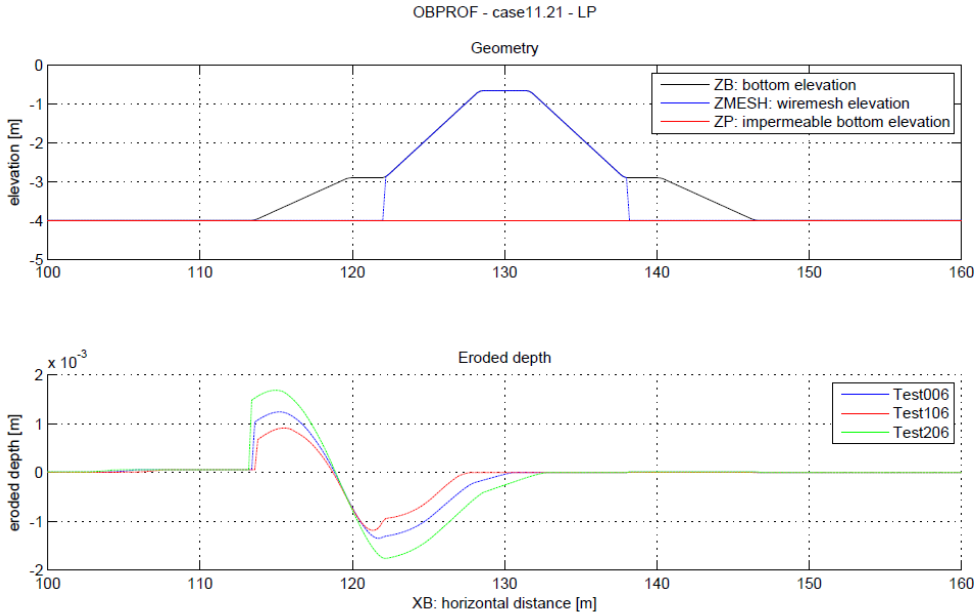

APPENDIX B

Stones measurements for physical model

Stone: PA01: RED				
Max	300	4.83		
Min	119	3.56		
Avg	186	4.10		
Total	18617			
density	2.65			
	Model			
stone N°	Mass [g]	Dn [cm]	f	fcum
81	119	3.56	0.6%	1%
48	121	3.58	0.7%	1%
59	124	3.60	0.7%	2%
20	124	3.61	0.7%	3%
30	126	3.62	0.7%	3%
27	127	3.63	0.7%	4%
87	128	3.64	0.7%	5%
97	129	3.65	0.7%	5%
44	131	3.67	0.7%	6%
19	131	3.67	0.7%	7%
62	133	3.69	0.7%	7%
55	134	3.69	0.7%	8%
21	136	3.72	0.7%	9%
28	137	3.72	0.7%	10%
72	138	3.73	0.7%	10%
15	139	3.74	0.7%	11%
66	140	3.75	0.8%	12%
49	141	3.76	0.8%	13%
63	142	3.77	0.8%	13%
53	142	3.77	0.8%	14%
86	143	3.78	0.8%	15%
100	143	3.78	0.8%	16%
43	144	3.79	0.8%	17%
23	145	3.79	0.8%	17%
54	145	3.80	0.8%	18%
40	146	3.80	0.8%	19%
94	146	3.80	0.8%	20%
60	146	3.80	0.8%	20%
2	146	3.81	0.8%	21%
96	148	3.83	0.8%	22%
84	148	3.83	0.8%	23%
29	149	3.83	0.8%	24%
17	150	3.84	0.8%	24%
9	152	3.85	0.8%	25%

52	152	3.86	0.8%	26%
93	152	3.86	0.8%	27%
76	154	3.87	0.8%	28%
51	156	3.89	0.8%	29%
82	156	3.89	0.8%	29%
38	157	3.90	0.8%	30%
24	158	3.91	0.8%	31%
70	163	3.95	0.9%	32%
16	165	3.96	0.9%	33%
61	165	3.97	0.9%	34%
4	167	3.98	0.9%	35%
64	169	3.99	0.9%	35%
73	170	4.00	0.9%	36%
3	173	4.02	0.9%	37%
56	176	4.05	0.9%	38%
12	176	4.05	0.9%	39%
5	178	4.06	1.0%	40%
69	180	4.08	1.0%	41%
67	181	4.08	1.0%	42%
68	187	4.13	1.0%	43%
80	189	4.14	1.0%	44%
50	191	4.16	1.0%	45%
8	193	4.17	1.0%	46%
75	193	4.18	1.0%	47%
37	193	4.18	1.0%	48%
11	196	4.20	1.1%	49%
32	200	4.23	1.1%	50%
90	202	4.24	1.1%	51%
58	203	4.25	1.1%	53%
36	203	4.25	1.1%	54%
34	206	4.27	1.1%	55%
98	209	4.29	1.1%	56%
77	209	4.29	1.1%	57%
92	210	4.30	1.1%	58%
6	210	4.30	1.1%	59%
83	213	4.31	1.1%	60%
74	213	4.31	1.1%	62%
89	214	4.32	1.1%	63%
47	215	4.33	1.2%	64%
26	215	4.33	1.2%	65%
46	217	4.34	1.2%	66%
41	219	4.36	1.2%	67%
35	225	4.40	1.2%	69%

31	231	4.43	1.2%	70%
85	233	4.44	1.2%	71%
65	234	4.45	1.3%	72%
95	235	4.46	1.3%	74%
45	237	4.47	1.3%	75%
79	237	4.47	1.3%	76%
91	241	4.50	1.3%	77%
99	242	4.50	1.3%	79%
7	243	4.51	1.3%	80%
25	244	4.52	1.3%	81%
1	246	4.53	1.3%	83%
71	252	4.57	1.4%	84%
18	253	4.57	1.4%	85%
88	264	4.64	1.4%	87%
13	265	4.64	1.4%	88%
57	266	4.65	1.4%	90%
33	266	4.65	1.4%	91%
22	267	4.65	1.4%	92%
10	269	4.66	1.4%	94%
42	270	4.67	1.4%	95%
78	276	4.71	1.5%	97%
14	283	4.74	1.5%	98%
39	300	4.83	1.6%	100%

Stone: SA01: GREEN				
Max	162	3.80		
Min	100	3.24		
Avg	128	3.51		
Total	12787			
density	2.94			
	Model			
stone N°	Mass [g]	Dn [cm]	f	fcum
61	100	3.24	0.8%	1%
24	101	3.25	0.8%	2%
62	101	3.25	0.8%	2%
23	101	3.25	0.8%	3%
95	102	3.26	0.8%	4%
55	102	3.26	0.8%	5%
57	102	3.27	0.8%	6%
33	103	3.27	0.8%	6%
67	103	3.27	0.8%	7%
85	103	3.28	0.8%	8%
39	105	3.29	0.8%	9%
88	106	3.31	0.8%	10%
31	107	3.32	0.8%	10%
92	108	3.32	0.8%	11%
77	108	3.33	0.8%	12%
16	109	3.33	0.9%	13%
6	109	3.34	0.9%	14%
60	109	3.34	0.9%	15%
68	110	3.34	0.9%	16%
9	110	3.34	0.9%	16%
86	111	3.36	0.9%	17%
75	112	3.36	0.9%	18%
38	113	3.37	0.9%	19%
14	114	3.38	0.9%	20%
5	114	3.38	0.9%	21%
99	115	3.39	0.9%	22%
53	115	3.39	0.9%	23%
93	116	3.40	0.9%	24%
26	116	3.41	0.9%	24%
89	116	3.41	0.9%	25%
83	118	3.42	0.9%	26%
100	118	3.42	0.9%	27%
36	118	3.42	0.9%	28%
11	118	3.43	0.9%	29%

78	119	3.43	0.9%	30%
81	119	3.43	0.9%	31%
49	120	3.44	0.9%	32%
29	121	3.45	0.9%	33%
69	121	3.46	0.9%	34%
56	121	3.46	0.9%	35%
96	122	3.46	1.0%	36%
46	122	3.46	1.0%	37%
25	123	3.47	1.0%	38%
42	123	3.47	1.0%	39%
91	123	3.47	1.0%	39%
71	123	3.47	1.0%	40%
54	124	3.48	1.0%	41%
51	124	3.48	1.0%	42%
1	125	3.49	1.0%	43%
40	126	3.50	1.0%	44%
27	126	3.50	1.0%	45%
15	127	3.50	1.0%	46%
35	127	3.51	1.0%	47%
18	127	3.51	1.0%	48%
70	127	3.51	1.0%	49%
41	128	3.52	1.0%	50%
7	129	3.52	1.0%	51%
76	131	3.54	1.0%	52%
3	131	3.55	1.0%	53%
90	131	3.55	1.0%	54%
32	133	3.56	1.0%	55%
37	133	3.56	1.0%	56%
47	134	3.57	1.0%	57%
79	134	3.57	1.0%	59%
44	135	3.58	1.1%	60%
87	135	3.58	1.1%	61%
94	135	3.58	1.1%	62%
58	136	3.59	1.1%	63%
73	136	3.59	1.1%	64%
50	140	3.62	1.1%	65%
20	140	3.62	1.1%	66%
97	140	3.62	1.1%	67%
59	140	3.63	1.1%	68%
52	143	3.65	1.1%	69%
22	143	3.65	1.1%	70%
2	144	3.66	1.1%	72%
21	144	3.66	1.1%	73%

45	145	3.67	1.1%	74%
12	145	3.67	1.1%	75%
80	145	3.67	1.1%	76%
84	146	3.68	1.1%	77%
64	146	3.68	1.1%	78%
65	147	3.68	1.1%	80%
98	148	3.69	1.2%	81%
19	148	3.69	1.2%	82%
63	149	3.70	1.2%	83%
30	150	3.71	1.2%	84%
74	150	3.71	1.2%	85%
17	150	3.71	1.2%	87%
10	153	3.73	1.2%	88%
13	154	3.74	1.2%	89%
34	154	3.74	1.2%	90%
28	154	3.74	1.2%	91%
4	155	3.75	1.2%	93%
66	157	3.76	1.2%	94%
8	158	3.77	1.2%	95%
82	158	3.78	1.2%	96%
72	159	3.78	1.2%	97%
48	160	3.79	1.3%	99%
43	162	3.80	1.3%	100%

Stone: SA02: BLUE				
Max	181	3.89		
Min	152	3.67		
Avg	168	3.80		
Total	8413			
density	3.06			
	Model			
stone N°	Mass [g]	Dn [cm]	f	fcum
3	152	3.67	1.8%	2%
18	157	3.72	1.9%	4%
10	159	3.73	1.9%	6%
24	160	3.74	1.9%	7%
22	160	3.74	1.9%	9%
35	161	3.74	1.9%	11%
17	161	3.74	1.9%	13%
28	161	3.74	1.9%	15%
26	161	3.75	1.9%	17%
50	161	3.75	1.9%	19%
46	162	3.75	1.9%	21%
12	162	3.76	1.9%	23%
19	163	3.76	1.9%	25%
42	163	3.76	1.9%	27%
23	163	3.76	1.9%	29%
34	164	3.77	1.9%	31%
39	164	3.77	2.0%	32%
13	165	3.77	2.0%	34%
45	165	3.78	2.0%	36%
5	165	3.78	2.0%	38%
14	165	3.78	2.0%	40%
41	166	3.78	2.0%	42%
48	167	3.79	2.0%	44%
1	167	3.79	2.0%	46%
27	168	3.80	2.0%	48%
11	169	3.81	2.0%	50%
2	169	3.81	2.0%	52%
38	170	3.81	2.0%	54%
43	170	3.81	2.0%	56%
25	170	3.81	2.0%	58%
36	170	3.82	2.0%	60%
30	172	3.83	2.0%	62%
33	172	3.83	2.0%	64%
49	173	3.84	2.1%	66%

4	173	3.84	2.1%	69%
31	173	3.84	2.1%	71%
20	174	3.84	2.1%	73%
37	174	3.84	2.1%	75%
40	174	3.84	2.1%	77%
7	174	3.85	2.1%	79%
47	175	3.85	2.1%	81%
21	176	3.86	2.1%	83%
32	176	3.86	2.1%	85%
15	177	3.86	2.1%	87%
8	177	3.87	2.1%	89%
29	178	3.88	2.1%	91%
6	179	3.88	2.1%	94%
9	179	3.88	2.1%	96%
44	180	3.89	2.1%	98%
16	181	3.89	2.1%	100%

Stone: BF01_small				
Max	16	1.80		
Min	3	1.05		
Avg	9	1.46		
Total	863			
density	2.71			
	Model			
stone N°	Mass [g]	Dn [cm]	f	fcum
39	3.1	1.05	0.4%	0%
37	4.3	1.17	0.5%	1%
52	4.5	1.18	0.5%	1%
83	4.7	1.20	0.5%	2%
84	4.8	1.21	0.6%	2%
53	4.9	1.22	0.6%	3%
88	5.3	1.25	0.6%	4%
28	5.4	1.26	0.6%	4%
68	5.4	1.26	0.6%	5%
26	5.6	1.27	0.6%	6%
42	5.6	1.27	0.6%	6%
87	5.6	1.27	0.6%	7%
51	5.7	1.28	0.7%	8%
93	5.8	1.29	0.7%	8%
35	5.9	1.30	0.7%	9%
58	5.9	1.30	0.7%	10%
62	6.0	1.30	0.7%	10%
46	6.1	1.31	0.7%	11%
94	6.2	1.32	0.7%	12%
59	6.5	1.34	0.8%	12%
60	6.5	1.34	0.8%	13%
69	6.5	1.34	0.8%	14%
98	6.5	1.34	0.8%	15%
32	6.6	1.35	0.8%	15%
33	6.6	1.35	0.8%	16%
78	6.6	1.35	0.8%	17%
92	6.6	1.35	0.8%	18%
13	6.7	1.35	0.8%	19%
44	6.7	1.35	0.8%	19%
80	6.7	1.35	0.8%	20%
18	6.8	1.36	0.8%	21%
36	6.9	1.37	0.8%	22%
77	6.9	1.37	0.8%	22%
64	7.0	1.37	0.8%	23%

45	7.1	1.38	0.8%	24%
65	7.1	1.38	0.8%	25%
89	7.2	1.39	0.8%	26%
4	7.4	1.40	0.9%	27%
91	7.4	1.40	0.9%	27%
11	7.5	1.40	0.9%	28%
47	7.5	1.40	0.9%	29%
72	7.5	1.40	0.9%	30%
95	7.5	1.40	0.9%	31%
3	7.7	1.42	0.9%	32%
14	7.7	1.42	0.9%	33%
97	7.8	1.42	0.9%	34%
24	8.2	1.45	1.0%	35%
25	8.2	1.45	1.0%	36%
50	8.2	1.45	1.0%	36%
86	8.2	1.45	1.0%	37%
40	8.4	1.46	1.0%	38%
55	8.4	1.46	1.0%	39%
61	8.4	1.46	1.0%	40%
41	8.5	1.46	1.0%	41%
82	8.5	1.46	1.0%	42%
54	8.6	1.47	1.0%	43%
7	8.7	1.48	1.0%	44%
17	8.7	1.48	1.0%	45%
5	8.8	1.48	1.0%	46%
96	8.8	1.48	1.0%	47%
2	8.9	1.49	1.0%	48%
100	9.0	1.49	1.0%	49%
10	9.1	1.50	1.1%	51%
70	9.1	1.50	1.1%	52%
15	9.2	1.50	1.1%	53%
57	9.3	1.51	1.1%	54%
34	9.5	1.52	1.1%	55%
56	9.6	1.52	1.1%	56%
76	9.6	1.52	1.1%	57%
73	9.8	1.53	1.1%	58%
74	9.8	1.53	1.1%	59%
90	10.1	1.55	1.2%	60%
38	10.2	1.56	1.2%	62%
79	10.3	1.56	1.2%	63%
12	10.6	1.58	1.2%	64%
19	10.6	1.58	1.2%	65%
43	10.6	1.58	1.2%	67%

31	10.7	1.58	1.2%	68%
66	10.8	1.59	1.3%	69%
20	11.0	1.60	1.3%	70%
16	11.1	1.60	1.3%	72%
22	11.1	1.60	1.3%	73%
67	11.1	1.60	1.3%	74%
85	11.1	1.60	1.3%	75%
21	11.2	1.60	1.3%	77%
49	11.2	1.60	1.3%	78%
71	11.2	1.60	1.3%	79%
27	11.7	1.63	1.4%	81%
99	11.7	1.63	1.4%	82%
30	12.1	1.65	1.4%	83%
63	12.4	1.66	1.4%	85%
6	12.8	1.68	1.5%	86%
81	13.6	1.71	1.6%	88%
9	13.8	1.72	1.6%	90%
1	13.9	1.72	1.6%	91%
48	14.3	1.74	1.7%	93%
75	15.1	1.77	1.7%	95%
29	15.5	1.79	1.8%	96%
23	15.6	1.79	1.8%	98%
8	15.7	1.80	1.8%	100%

Stone: BF02_large				
Max	27	2.14		
Min	3	1.02		
Avg	15	1.75		
Total	1512			
density	2.72			
	Model			
stone N°	Mass [g]	Dn [cm]	f	fcum
63	2.88	1.02	0.2%	0%
70	9	1.46	0.6%	1%
98	9	1.47	0.6%	1%
27	9	1.51	0.6%	2%
65	9	1.51	0.6%	3%
92	10	1.52	0.6%	3%
64	10	1.55	0.7%	4%
6	10	1.55	0.7%	5%
94	10	1.56	0.7%	5%
1	11	1.57	0.7%	6%
88	11	1.58	0.7%	7%
100	11	1.58	0.7%	7%
96	11	1.59	0.7%	8%
74	11	1.59	0.7%	9%
46	11	1.60	0.7%	10%
71	11	1.60	0.7%	10%
18	11	1.60	0.7%	11%
67	11	1.61	0.7%	12%
89	11	1.61	0.7%	12%
51	11	1.61	0.8%	13%
80	11	1.61	0.8%	14%
82	11	1.61	0.8%	15%
37	12	1.62	0.8%	16%
38	12	1.63	0.8%	16%
77	12	1.63	0.8%	17%
40	12	1.64	0.8%	18%
73	12	1.64	0.8%	19%
62	12	1.64	0.8%	19%
3	12	1.65	0.8%	20%
15	12	1.65	0.8%	21%
97	12	1.65	0.8%	22%
55	13	1.66	0.8%	23%
58	13	1.66	0.8%	24%
41	13	1.67	0.8%	24%

60	13	1.68	0.8%	25%
61	13	1.68	0.8%	26%
99	13	1.68	0.8%	27%
8	13	1.68	0.9%	28%
59	13	1.68	0.9%	29%
13	13	1.69	0.9%	29%
42	13	1.69	0.9%	30%
72	13	1.70	0.9%	31%
93	14	1.71	0.9%	32%
84	14	1.71	0.9%	33%
90	14	1.72	0.9%	34%
75	14	1.72	0.9%	35%
22	14	1.73	0.9%	36%
45	14	1.73	0.9%	37%
91	14	1.73	0.9%	38%
76	14	1.73	0.9%	39%
20	15	1.76	1.0%	40%
32	15	1.76	1.0%	41%
53	15	1.76	1.0%	42%
66	15	1.76	1.0%	43%
11	15	1.77	1.0%	44%
83	16	1.79	1.0%	45%
10	16	1.80	1.0%	46%
30	16	1.80	1.0%	47%
56	16	1.80	1.0%	48%
29	16	1.80	1.1%	49%
33	16	1.80	1.1%	50%
36	16	1.80	1.1%	51%
5	16	1.81	1.1%	52%
81	16	1.81	1.1%	53%
9	16	1.82	1.1%	54%
21	16	1.82	1.1%	55%
78	17	1.82	1.1%	56%
26	17	1.83	1.1%	57%
19	17	1.84	1.1%	58%
4	17	1.85	1.1%	60%
39	17	1.85	1.1%	61%
28	17	1.86	1.2%	62%
68	18	1.86	1.2%	63%
17	18	1.87	1.2%	64%
48	18	1.87	1.2%	65%
85	18	1.87	1.2%	67%
14	18	1.88	1.2%	68%

2	18	1.88	1.2%	69%
47	18	1.88	1.2%	70%
52	19	1.90	1.2%	71%
23	19	1.91	1.2%	73%
24	19	1.91	1.2%	74%
86	19	1.91	1.2%	75%
54	19	1.92	1.3%	76%
7	19	1.92	1.3%	78%
50	19	1.92	1.3%	79%
16	19	1.92	1.3%	80%
35	20	1.93	1.3%	82%
79	20	1.94	1.3%	83%
95	20	1.95	1.3%	84%
49	21	1.96	1.4%	86%
25	21	1.96	1.4%	87%
31	22	2.00	1.4%	88%
87	23	2.03	1.5%	90%
43	24	2.06	1.6%	91%
44	25	2.10	1.7%	93%
12	26	2.11	1.7%	95%
34	26	2.12	1.7%	96%
69	27	2.14	1.8%	98%
57	27	2.14	1.8%	100%

APPENDIX C

Measured profiles of the physical model

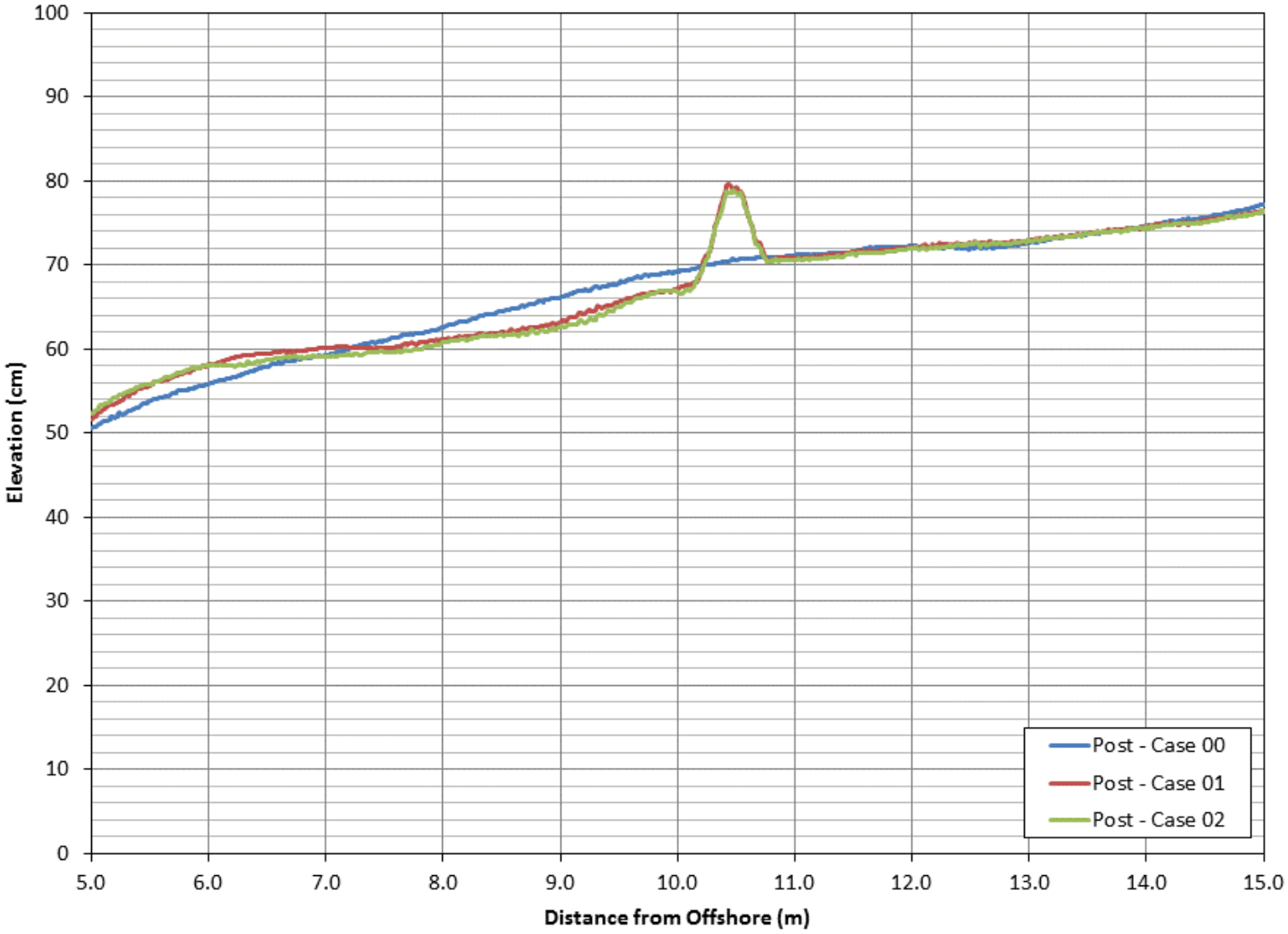
Elevation (cm)
100
90
80
70
60
50
40
30
20
10
0
5.0
6.0
7.0
8.0
9.0
10.0
11.0
12.0
13.0
14.0
15.0
Distance from Offshore (m)
Post - Case 00
Post - Case 01
Post - Case 02

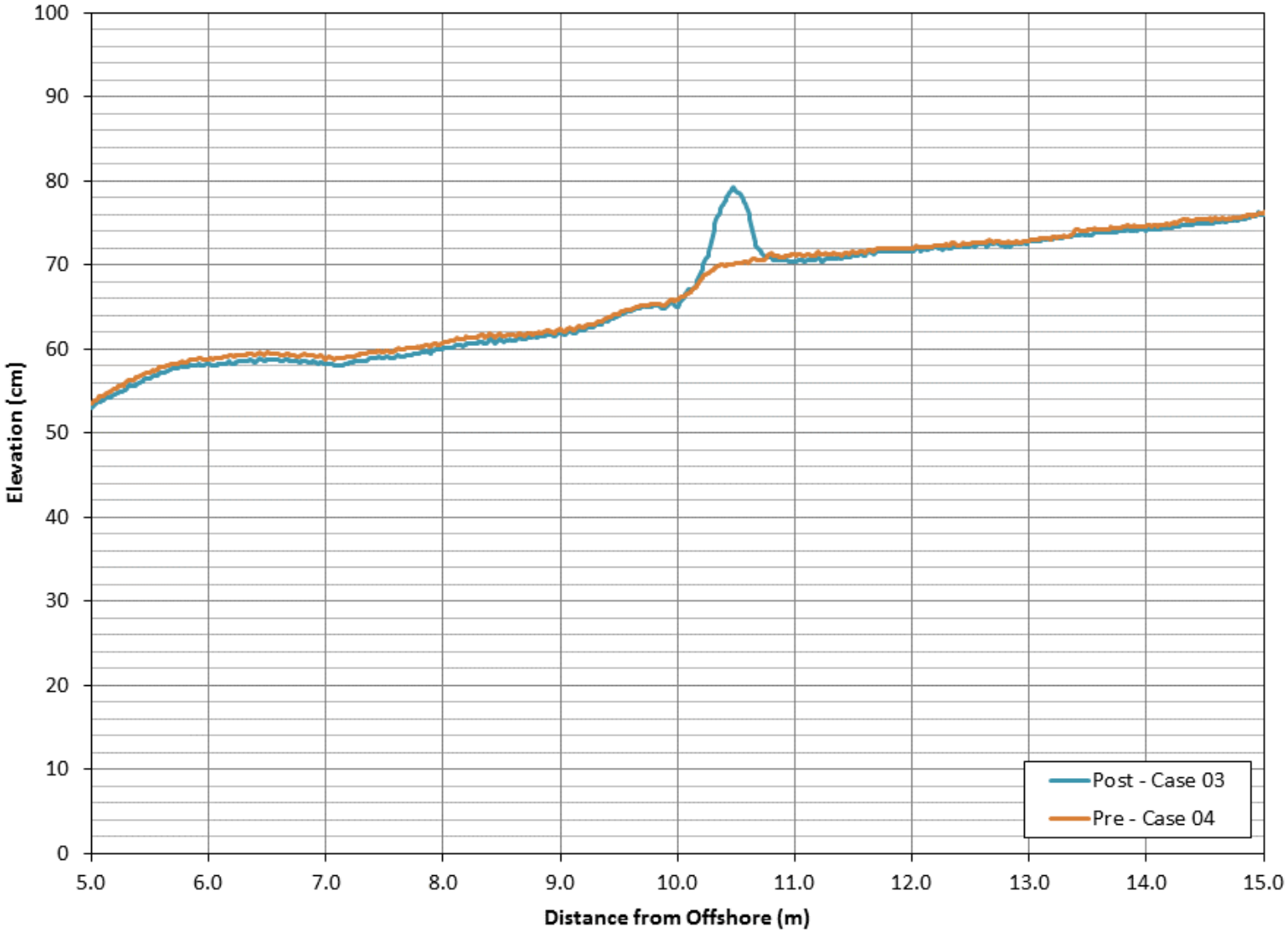
100
90
80
70
60
50
40
30
20
10
0
Elevation (cm)
5.0
6.0
7.0
8.0
9.0
10.0
11.0
12.0
13.0
14.0
15.0
Distance from Offshore (m)
Post - Case 03
Pre - Case 04

APPENDIX D

Results of hydrodynamic measurements of the physical model

Case 00 Tables

Case 00 incident wave characteristics at WG1 (x = 0 m).

Run	H_{mo} (cm)	H_{rms} (cm)	H_s (cm)	T_p (s)	T_s (s)	R
T1D1_1	18.43	13.03	17.92	2.03	1.82	0.12
T1D2_1	18.01	12.73	17.27	1.88	1.77	0.12
T2D1_1	18.75	13.26	18.59	2.68	2.25	0.13
T2D2_1	18.07	12.78	17.79	2.81	2.27	0.12

Case 00 mean free-surface elevation $\overline{\eta}$ (cm) at six wave gauge locations.

Run	WG1	WG2	WG3	WG4	WG5	WG6
T1D1_1	-0.23	-0.17	-0.22	-0.25	0.51	0.91
T1D2_1	-0.17	-0.10	-0.18	-0.22	0.33	0.63
T2D1_1	-0.26	-0.15	-0.27	-0.31	0.70	1.09
T2D2_1	-0.21	-0.16	-0.24	-0.30	0.37	0.73

Case 00 free-surface standard deviation σ_η (cm) at six wave gauge locations.

Run	WG1	WG2	WG3	WG4	WG5	WG6
T1D1_1	4.48	4.48	4.48	4.39	2.33	1.70
T1D2_1	4.40	4.40	4.37	4.20	2.56	1.82
T2D1_1	4.61	4.57	4.60	4.64	2.43	1.83
T2D2_1	4.48	4.49	4.48	4.48	2.79	2.01

Case 00 mean cross-shore $\overline{u}$ and its standard deviation σ_u of the red Vectrino co-located with WG5 at x = 10.10 m and blue Vectrino co-located with WG6 at x = 11.97 m.

Run	Red Vectrino at WG5		Blue Vectrino at WG6	
	$\overline{u}$ (cm/s)	σ_u (cm/s)	$\overline{u}$ (cm/s)	σ_u (cm/s)
T1D1_1	-6.85	18.06	-4.13	14.83
T1D2_1	NR	NR	-5.09	14.68
T2D1_1	-7.75	18.28	-4.67	16.10
T2D2_1	-7.46	19.81	-4.96	16.88

Case 01 – T1D1 Tables

Case 01 (T1D1) incident wave characteristics at WG1 (x = 0 m).

Run	H_{mo} (cm)	H_{rms} (cm)	H_s (cm)	T_p (s)	T_s (s)	R
T1D1_1	17.25	12.20	16.67	2.03	1.82	0.18
T1D1_2	17.30	12.23	16.75	2.03	1.81	0.17
T1D1_3	17.41	12.31	16.88	2.03	1.81	0.17

Case 01 (T1D1) mean free-surface elevation $\bar{\eta}$ (cm) at six wave gauge locations.

Run	WG1	WG2	WG3	WG4	WG5	WG6
T1D1_1	-0.29	-0.22	-0.25	-0.34	NR	NR
T1D1_2	-0.28	-0.22	-0.26	-0.35	NR	NR
T1D1_3	-0.26	-0.15	-0.27	-0.36	NR	NR

NR implies "not reliable" data

Case 01 (T1D1) free-surface standard deviation σ_η (cm) at six wave gauge locations.

Run	WG1	WG2	WG3	WG4	WG5	WG6
T1D1_1	4.20	4.15	4.25	4.24	NR	NR
T1D1_2	4.22	4.17	4.26	4.26	NR	NR
T1D1_3	4.25	4.20	4.28	4.27	NR	NR

NR implies "not reliable" data

Case 01 (T1D1) mean cross-shore $\bar{u}$ and its standard deviation σ_u of the red Vectrino co-located with WG5 at x = 10.10 m and blue Vectrino co-located with WG6 at x = 11.97 m.

Run	**Red Vectrino at WG5**		**Blue Vectrino at WG6**	
	$\bar{u}$ **(*cm/s*)**	σ_u **(*cm/s*)**	$\bar{u}$ **(*cm/s*)**	σ_u **(*cm/s*)**
T1D1_1	-2.48	17.11	-1.55	10.64
T1D1_2	-2.34	17.07	-1.59	10.60
T1D1_3	-2.78	17.45	-1.95	10.72

Case 01 – T2D1 Tables

Case 01 (T2D1) incident wave characteristics at WG1 (x = 0 m).

Run	H_{mo} (cm)	H_{rms} (cm)	H_s (cm)	T_p (s)	T_s (s)	R
T2D1_1	17.28	12.22	17.10	2.68	2.24	0.16
T2D1_2	17.47	12.35	17.24	2.68	2.24	0.17
T2D1_3	17.48	12.36	17.33	2.68	2.25	0.16
T2D1_4	17.53	12.40	17.26	2.68	2.23	0.17
T2D1_5	17.56	12.42	17.20	2.68	2.23	0.16
T2D1_6	17.56	12.41	17.29	2.68	2.21	0.16
T2D1_7	17.47	12.36	17.17	2.68	2.24	0.17
T2D1_8	17.47	12.35	17.28	2.68	2.26	0.16
T2D1_9	17.48	12.36	17.27	2.68	2.28	0.18
Run	H_{mo} (cm)	H_{rms} (cm)	H_s (cm)	T_p (s)	T_s (s)	R
T2D1_1	17.28	12.22	17.10	2.68	2.24	0.16
T2D1_2	17.47	12.35	17.24	2.68	2.24	0.17
T2D1_3	17.48	12.36	17.33	2.68	2.25	0.16
T2D1_4	17.53	12.40	17.26	2.68	2.23	0.17
T2D1_5	17.56	12.42	17.20	2.68	2.23	0.16
T2D1_6	17.56	12.41	17.29	2.68	2.21	0.16
T2D1_7	17.47	12.36	17.17	2.68	2.24	0.17
T2D1_8	17.47	12.35	17.28	2.68	2.26	0.16
T2D1_9	17.48	12.36	17.27	2.68	2.28	0.18

Case 01 (T2D1) mean free-surface elevation $\overline{\eta}$ (cm) at six wave gauge locations.

Run	WG1	WG2	WG3	WG4	WG5	WG6
T2D1_1	-0.34	-0.29	-0.29	-0.40	0.39	1.89
T2D1_2	-0.34	-0.30	-0.32	-0.41	0.39	1.89

T2D1_3	-0.33	-0.28	-0.33	-0.42	0.38	1.88
T2D1_4	-0.33	-0.28	-0.35	-0.43	0.36	1.89
T2D1_5	-0.33	-0.29	-0.36	-0.43	0.34	1.88
T2D1_6	-0.34	-0.30	-0.37	-0.43	0.32	1.87
T2D1_7	-0.31	-0.29	-0.38	-0.43	0.32	1.86
T2D1_8	-0.31	-0.29	-0.39	-0.44	0.30	1.87
T2D1_9	-0.29	-0.31	-0.39	-0.44	0.30	1.87

Case 01 (T2D1) free-surface standard deviation σ_η (*cm*) at six wave gauge locations.

Run	WG1	WG2	WG3	WG4	WG5	WG6
T2D1_1	4.22	4.19	4.27	4.31	2.55	1.36
T2D1_2	4.25	4.21	4.31	4.33	2.55	1.36
T2D1_3	4.26	4.24	4.32	4.35	2.56	1.35
T2D1_4	4.27	4.25	4.34	4.36	2.59	1.37
T2D1_5	4.28	4.26	4.33	4.37	2.59	1.36
T2D1_6	4.28	4.27	4.32	4.35	2.58	1.37
T2D1_7	4.25	4.24	4.30	4.38	2.59	1.37
T2D1_8	4.25	4.25	4.31	4.37	2.59	1.38
T2D1_9	4.26	4.24	4.31	4.37	2.60	1.38

Case 01 (T2D1) mean cross-shore $\bar{u}$ and its standard deviation σ_u of the red Vectrino co-located with WG5 at x = 10.10 *m* and blue Vectrino co-located with WG6 at x = 11.97 *m*.

Run	Red Vectrino at WG5		Blue Vectrino at WG6	
	$\bar{u}$ (*cm/s*)	σ_u (*cm/s*)	$\bar{u}$ (*cm/s*)	σ_u (*cm/s*)
T2D1_1	-3.53	17.69	-2.28	11.45
T2D1_2	-4.03	17.58	NR	NR
T2D1_3	-4.28	17.17	-1.73	11.52
T2D1_4	-4.80	17.56	NR	NR
T2D1_5	-4.51	17.51	-1.94	11.59
T2D1_6	NR	NR	NR	NR
T2D1_7	-4.03	18.07	-2.01	11.65
T2D1_8	NR	NR	-1.96	11.63
T2D1_9	-3.97	17.38	-2.29	11.45

NR implies "not reliable" data

Case 01 – T2D2 Tables

Case 01 (T2D2) incident wave characteristics at WG1 (x = 0 m).

Run	H_{mo} (cm)	H_{rms} (cm)	H_s (cm)	T_p (s)	T_s (s)	R
T2D2_1	16.78	11.87	16.32	2.81	2.26	0.15
T2D2_2	16.95	11.99	16.36	2.81	2.25	0.15
T2D2_3	17.04	12.05	16.65	2.81	2.27	0.15
T2D2_4	17.10	12.09	16.65	2.81	2.29	0.15
T2D2_5	17.18	12.14	16.83	2.81	2.23	0.16
T2D2_6	17.08	12.07	16.57	2.81	2.24	0.15
T2D2_7	17.06	12.07	16.62	2.81	2.27	0.15
T2D2_8	17.05	12.06	16.66	2.81	2.27	0.15
T2D2_9	17.05	12.05	16.67	2.81	2.27	0.16

Case 01 (T2D2) mean free-surface elevation $\overline{\boldsymbol{\eta}}$ (cm) at six wave gauge locations.

Run	WG1	WG2	WG3	WG4	WG5	WG6
T2D2_1	-0.35	-0.28	-0.21	-0.34	0.00	1.37
T2D2_2	-0.36	-0.30	-0.23	-0.41	-0.04	1.36
T2D2_3	-0.36	-0.30	-0.24	-0.42	-0.02	1.37
T2D2_4	-0.38	-0.30	-0.26	-0.45	-0.05	1.35
T2D2_5	-0.37	-0.29	-0.26	-0.44	-0.06	1.36
T2D2_6	-0.36	-0.28	-0.27	-0.45	-0.08	1.34
T2D2_7	-0.36	-0.26	-0.26	-0.45	-0.08	1.33
T2D2_8	-0.35	-0.28	-0.27	-0.45	-0.10	1.32
T2D2_9	-0.34	-0.28	-0.27	-0.44	-0.10	1.33

Case 01 (T2D2) free-surface standard deviation σ_η (*cm*) at six wave gauge locations.

Run	WG1	WG2	WG3	WG4	WG5	WG6
T2D2_1	4.13	4.15	4.20	4.29	2.95	1.63
T2D2_2	4.16	4.18	4.24	4.30	2.97	1.64
T2D2_3	4.18	4.21	4.27	4.32	2.97	1.65
T2D2_4	4.20	4.23	4.28	4.32	2.95	1.65
T2D2_5	4.20	4.23	4.30	4.33	2.97	1.66
T2D2_6	4.18	4.23	4.27	4.30	2.98	1.64
T2D2_7	4.18	4.22	4.28	4.30	3.00	1.64
T2D2_8	4.17	4.20	4.27	4.29	2.99	1.64
T2D2_9	4.18	4.20	4.27	4.29	3.00	1.65

Case 01 (T2D2) mean cross-shore $\overline{u}$ and its standard deviation σ_u of the red Vectrino co-located with WG5 at x = 10.10 *m* and blue Vectrino co-located with WG6 at x = 11.97 *m*.

Run	Red Vectrino at WG5		Blue Vectrino at WG6	
	$\overline{u}$ (*cm/s*)	σ_u (*cm/s*)	$\overline{u}$ (*cm/s*)	σ_u (*cm/s*)
T2D2_1	-3.07	17.97	NR	NR
T2D2_2	-2.55	19.19	-3.72	12.73
T2D2_3	NR	NR	-2.66	12.76
T2D2_4	-1.99	18.19	-3.23	12.87
T2D2_5	-2.55	18.95	-3.12	12.79
T2D2_6	-1.78	18.72	-3.13	12.81
T2D2_7	-2.79	18.74	-3.28	12.57
T2D2_8	-1.80	17.99	NR	NR
T2D2_9	NR	NR	NR	NR

NR implies "not reliable" data

Case 02 – T3D3 + T1D3 Tables

Case 02 incident wave characteristics at WG1 (x = 0 m).

Run	H_{mo} (cm)	H_{rms} (cm)	H_s (cm)	T_p (s)	T_s (s)	R
T3D3_1	4.05	2.86	3.92	1.22	1.07	0.24
T1D3_1	17.36	12.28	17.09	2.03	1.80	0.22
T1D3_2	17.48	12.36	17.23	2.03	1.81	0.22
T1D3_3	17.56	12.41	17.25	2.03	1.82	0.22
T1D3_4	17.58	12.43	17.33	2.03	1.81	0.23
T1D3_5	17.63	12.47	17.42	2.03	1.80	0.22

Case 02 mean free-surface elevation $\overline{\eta}$ (cm) at six wave gauge locations.

Run	WG1	WG2	WG3	WG4	WG5	WG6
T3D3_1	-0.06	-0.09	-0.08	-0.07	NR	NR
T1D3_1	-0.39	-0.26	-0.42	-0.49	NR	NR
T1D3_2	-0.37	-0.24	-0.43	-0.50	NR	NR
T1D3_3	-0.36	-0.22	-0.44	-0.50	NR	NR
T1D3_4	-0.35	-0.18	-0.45	-0.50	NR	NR
T1D3_5	-0.34	-0.18	-0.45	-0.50	NR	NR

NR implies "not reliable" data

Case 02 free-surface standard deviation σ_η (*cm*) at six wave gauge locations.

Run	WG1	WG2	WG3	WG4	WG5	WG6
T3D3_1	1.05	1.11	1.03	0.97	NR	NR
T1D3_1	4.31	4.13	4.35	4.38	NR	NR
T1D3_2	4.34	4.15	4.38	4.40	NR	NR
T1D3_3	4.35	4.18	4.39	4.42	NR	NR
T1D3_4	4.37	4.16	4.41	4.42	NR	NR
T1D3_5	4.37	4.18	4.42	4.42	NR	NR

NR implies "not reliable" data

Case 02 mean cross-shore $\bar{u}$ and its standard deviation σ_u of the red Vectrino co-located with WG5 at x = 10.10 *m* and blue Vectrino co-located with WG6 at x = 11.97 *m*.

Run	Red Vectrino at WG5		Blue Vectrino at WG6	
	$\bar{u}$ (*cm/s*)	σ_u (*cm/s*)	$\bar{u}$ (*cm/s*)	σ_u (*cm/s*)
T3D3_1	-0.04	7.90	-0.19	4.48
T1D3_1	-3.30	17.80	-1.69	9.46
T1D3_2	-2.21	17.60	NR	NR
T1D3_3	-2.88	17.22	-1.71	9.68
T1D3_4	-2.28	17.93	-2.20	9.64
T1D3_5	3.72	18.55	-2.31	9.79

NR implies "not reliable" data

Case 03 – T3D3 + T4D3 + T1D3 Tables

Case 03 incident wave characteristics at WG1 (x = 0 m).

Run	H_{mo} (cm)	H_{rms} (cm)	H_s (cm)	T_p (s)	T_s (s)	R
T3D3_1	3.86	2.73	3.75	1.22	1.08	0.22
T4D3_1	5.12	3.62	4.94	1.41	1.20	0.23
T1D3_1	17.25	12.20	16.81	2.03	1.81	0.18
T1D3_2	17.34	12.26	16.92	2.03	1.81	0.17
T1D3_3	17.44	12.33	16.95	2.03	1.81	0.17
T1D3_4	17.47	12.35	17.09	2.03	1.81	0.18
T1D3_5	17.41	12.31	16.81	2.03	1.81	0.18
T1D3_6	17.40	12.31	16.92	2.03	1.82	0.17
T1D1_1	17.32	12.25	16.74	2.03	1.80	0.16
T1D1_2	17.38	12.29	16.76	2.03	1.81	0.17
T1D1_3	17.38	12.29	16.82	2.03	1.81	0.16
T1D2_1	16.54	11.70	15.94	1.88	1.78	0.17
T1D2_2	16.48	11.65	15.96	1.88	1.80	0.17
T1D2_3	16.56	11.77	15.96	1.88	1.77	0.17

Case 03 mean free-surface elevation $\overline{\boldsymbol{\eta}}$ (*cm*) at six wave gauge locations.

Run	WG1	WG2	WG3	WG4	WG5	WG6
T3D3_1	-0.05	-0.04	-0.02	-0.06	-0.08	0.42
T4D3_1	-0.09	-0.08	-0.04	-0.10	-0.13	0.72
T1D3_1	-0.40	-0.36	-0.29	-0.46	0.19	2.31
T1D3_2	-0.41	-0.37	-0.30	-0.49	0.17	2.30
T1D3_3	-0.42	-0.37	-0.31	-0.50	0.16	2.29
T1D3_4	-0.42	-0.36	-0.31	-0.50	0.14	2.28
T1D3_5	-0.41	-0.35	-0.30	-0.50	0.13	2.29
T1D3_6	-0.42	-0.34	-0.31	-0.51	0.13	2.29
T1D1_1	-0.31	-0.27	-0.33	-0.37	0.11	1.82
T1D1_2	-0.31	-0.26	-0.33	-0.37	0.10	1.82
T1D1_3	-0.31	-0.27	-0.34	-0.35	0.10	1.82
T1D2_1	-0.22	-0.17	-0.27	-0.30	-0.05	1.27
T1D2_2	-0.21	-0.16	-0.27	-0.31	-0.04	1.27
T1D2_3	-0.22	-0.15	-0.28	-0.32	-0.05	1.27

Case 03 free-surface standard deviation σ_η (*cm*) at six wave gauge locations.

Run	WG1	WG2	WG3	WG4	WG5	WG6
T3D3_1	1.00	0.98	1.00	0.91	0.81	0.48
T4D3_1	1.30	1.28	1.30	1.23	1.06	0.62
T1D3_1	4.19	4.14	4.26	4.25	2.39	1.32
T1D3_2	4.20	4.17	4.29	4.25	2.40	1.32
T1D3_3	4.23	4.19	4.31	4.27	2.43	1.35
T1D3_4	4.23	4.21	4.31	4.28	2.42	1.35
T1D3_5	4.22	4.19	4.31	4.27	2.43	1.35
T1D3_6	4.21	4.19	4.31	4.28	2.44	1.35
T1D1_1	4.19	4.21	4.26	4.23	2.63	1.53
T1D1_2	4.20	4.23	4.27	4.23	2.63	1.54
T1D1_3	4.21	4.23	4.27	4.23	2.64	1.56
T1D2_1	4.05	4.02	4.06	3.91	2.78	1.73
T1D2_2	4.04	4.00	4.06	3.92	2.79	1.74
T1D2_3	4.06	4.03	4.07	3.93	2.79	1.74

Case 03 mean cross-shore $\overline{u}$ and its standard deviation σ_u of the red Vectrino co-located with WG5 at x = 10.10 *m* and blue Vectrino co-located with WG6 at x = 11.97 *m*.

Run	Red Vectrino at WG5		Blue Vectrino at WG6	
	$\overline{u}$ (*cm/s*)	σ_u (*cm/s*)	$\overline{u}$ (*cm/s*)	σ_u (*cm/s*)
T3D3_1	NR	NR	-0.65	4.49
T4D3_1	-0.37	10.42	-0.56	5.54
T1D3_1	-2.61	18.75	-2.43	9.79
T1D3_2	-2.79	18.18	-2.50	9.95
T1D3_3	-2.29	17.45	-3.06	9.92
T1D3_4	-2.27	17.14	-2.39	10.10
T1D3_5	-2.40	17.54	-2.29	10.15
T1D3_6	-3.13	17.62	-1.89	10.09
T1D1_1	NR	NR	NR	NR
T1D1_2	-1.78	18.43	-3.20	11.26
T1D1_3	-1.31	17.68	-3.26	11.31
T1D2_1	NR	NR	NR	NR
T1D2_2	NR	NR	NR	NR
T1D2_3	NR	NR	NR	NR

NR implies "not reliable" data

Case 04 Tables

Case 04 incident wave characteristics at WG1 (x = 0 m).

Run	H_{mo} (cm)	H_{rms} (cm)	H_s (cm)	T_p (s)	T_s (s)	R
T3D3_1	3.79	2.68	3.66	1.22	1.08	0.12
T4D3_1	5.13	3.63	4.96	1.41	1.21	0.11
T1D3_1	17.50	12.37	17.14	2.03	1.83	0.13
T1D1_1	17.67	12.47	17.19	2.03	1.83	0.12
T1D2_1	16.74	11.84	16.04	1.88	1.78	0.12

Case 04 mean free-surface elevation $\overline{\eta}$ (cm) at six wave gauge locations.

Run	WG1	WG2	WG3	WG4	WG5	WG6
T3D3_1	0.03	0.07	-0.01	0.00	-0.08	-0.02
T4D3_1	0.04	0.08	-0.02	-0.01	-0.09	-0.01
T1D3_1	-0.16	-0.03	-0.21	-0.27	0.29	0.81
T1D1_1	-0.20	-0.16	-0.12	-0.26	0.20	0.65
T1D2_1	-0.17	-0.11	-0.14	-0.19	0.08	0.45

Case 04 free-surface standard deviation σ_η (cm) at six wave gauge locations.

Run	WG1	WG2	WG3	WG4	WG5	WG6
T3D3_1	0.97	0.96	0.93	0.89	0.91	0.92
T4D3_1	1.27	1.28	1.25	1.21	1.25	1.11
T1D3_1	4.24	4.24	4.26	4.24	2.47	1.65
T1D1_1	4.29	4.29	4.30	4.25	2.72	1.94
T1D2_1	4.07	4.06	4.10	3.98	2.84	2.22

Case 04 mean cross-shore $\overline{u}$ and its standard deviation σ_u of the red Vectrino co-located with WG5 at x = 10.10 m and blue Vectrino co-located with WG6 at x = 11.97 m.

Run	Red Vectrino at WG5		Blue Vectrino at WG6	
	$\overline{u}$ (cm/s)	σ_u (cm/s)	$\overline{u}$ (cm/s)	σ_u (cm/s)
T3D3_1	-0.16	6.43	-1.23	7.99
T4D3_1	-0.43	8.37	-2.04	9.30
T1D3_1	-3.89	16.44	-6.10	14.87
T1D1_1	-4.64	17.14	-4.68	15.81
T1D2_1	-4.61	17.61	-6.37	15.84

APPENDIX E

Physical model photographs and laser scan for damage estimation

Case 01 T1D1

Initial

Final

Initial

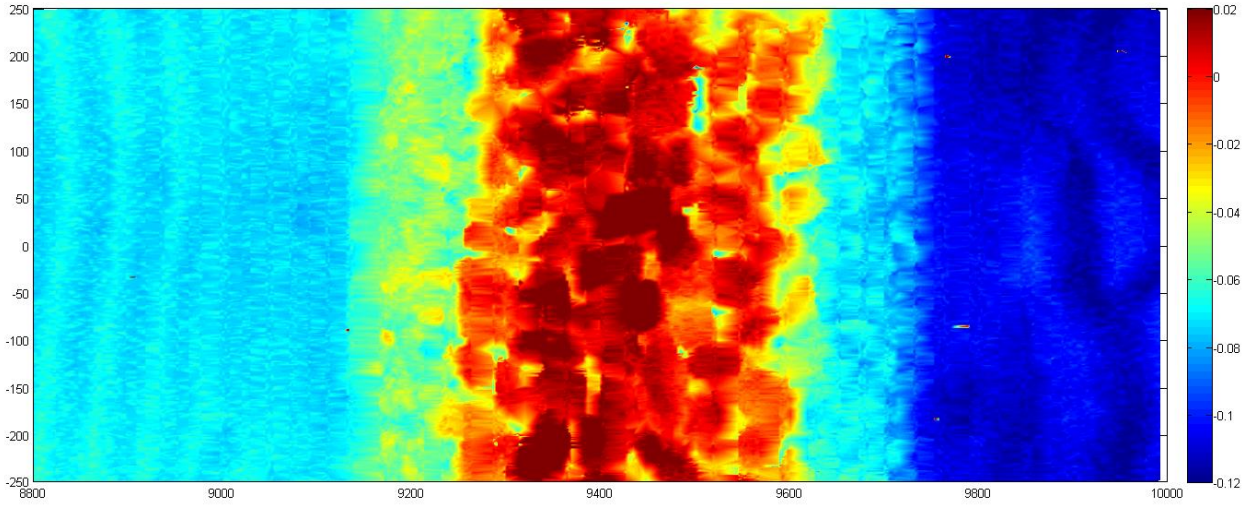

landward seaward

Final

Final scan was not taken since no stone displacement was seen.

Case 01 T2D1

Initial

Final

Initial

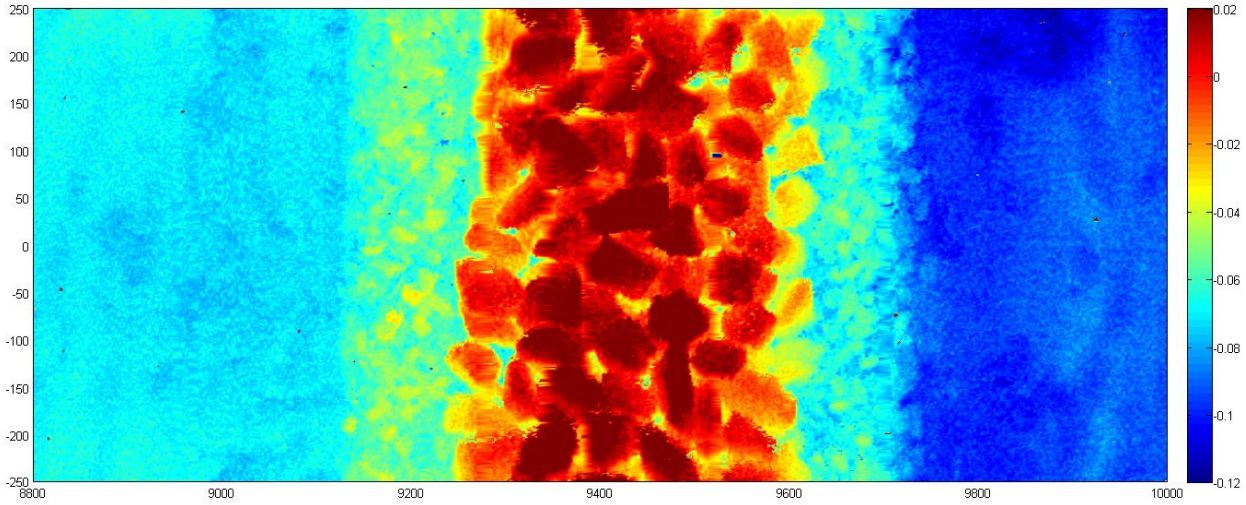

landward seaward

Final

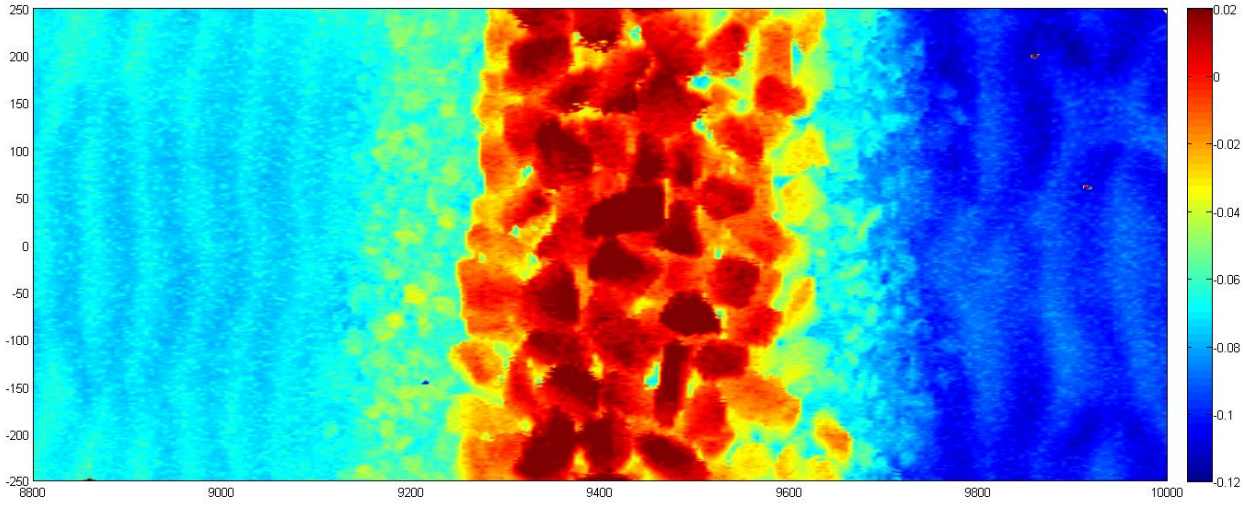

landward seaward

Case 01 T2D2

Initial

Final

Initial

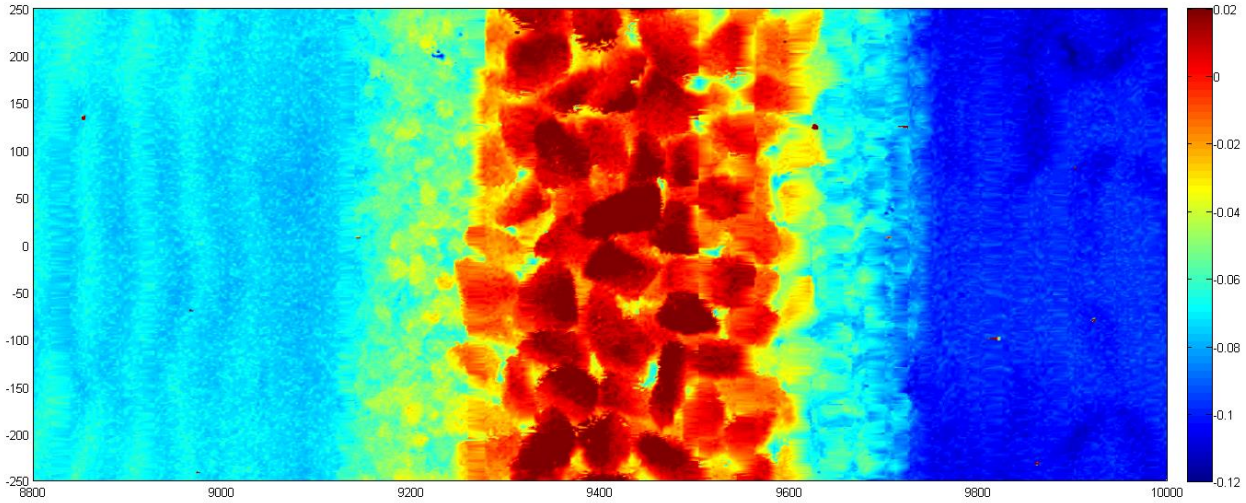

landward seaward

Final

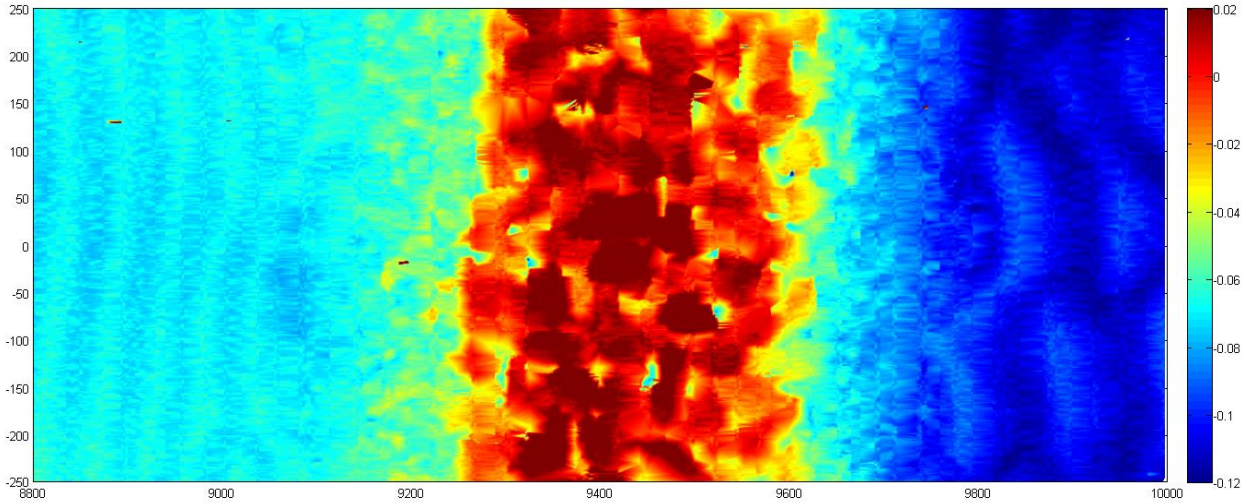

landward seaward

Case 02 T1D3

Initial

Final

Initial

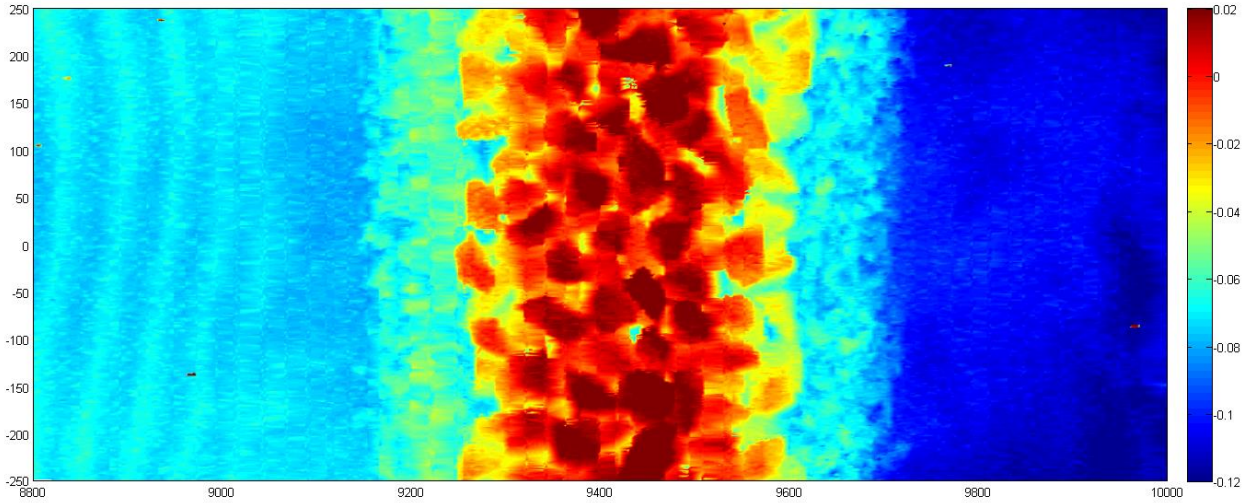

landward seaward

Final

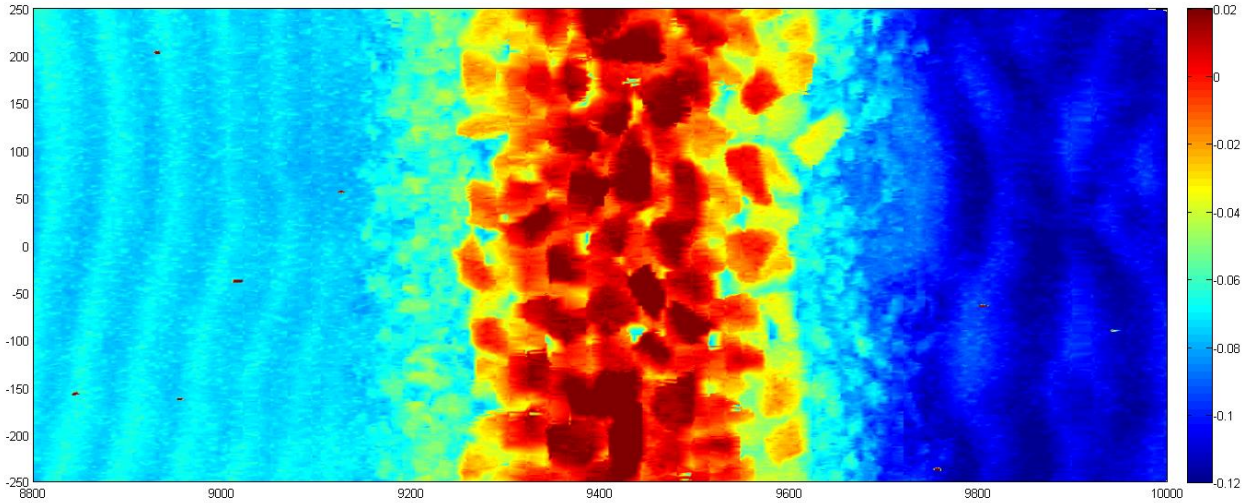

landward seaward

Case 03 T1D3+T1D1+T1D2

Initial

Final

Initial

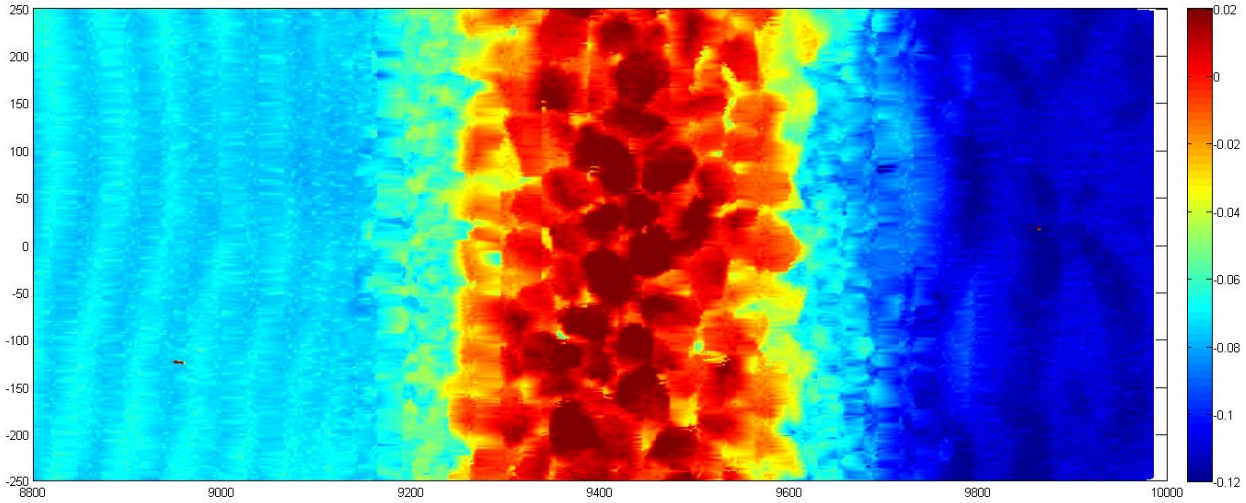

landward seaward

Final

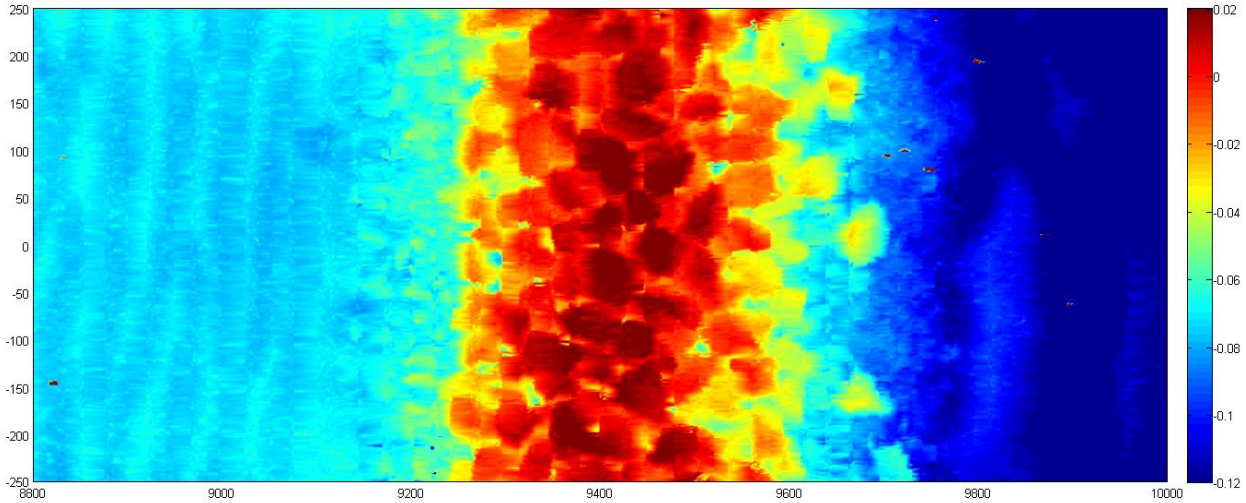

landward seaward

APPENDIX F

Results of numerical model for recommended design

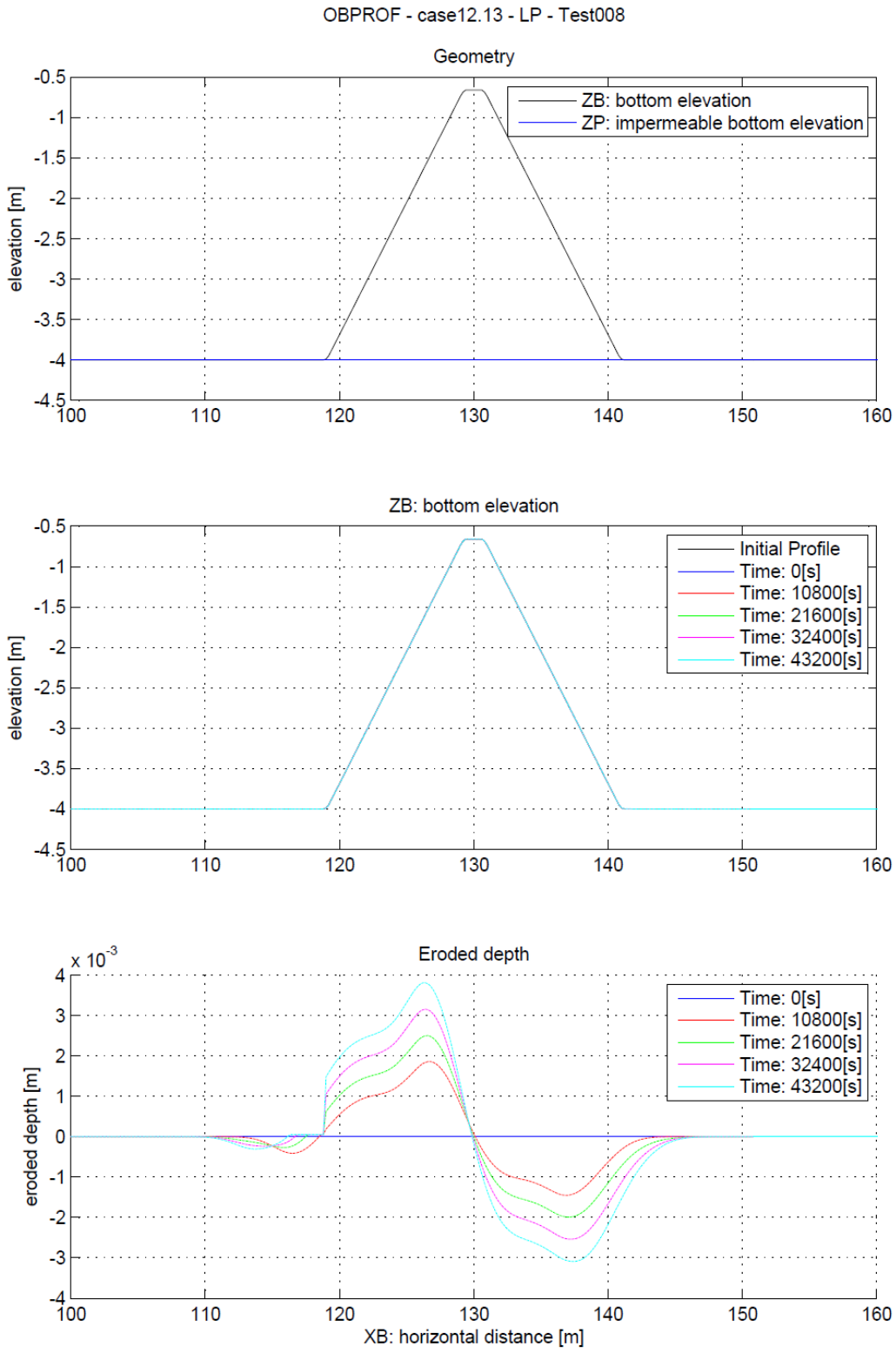
OBPROF - case12.13 - LP - Test008
Geometry
ZB: bottom elevation
ZP: impermeable bottom elevation
elevation [m]
ZB: bottom elevation
Initial Profile
Time: 0[s]
Time: 10800[s]
Time: 21600[s]
Time: 32400[s]
Time: 43200[s]
elevation [m]
Eroded depth
x 10^-3
Time: 0[s]
Time: 10800[s]
Time: 21600[s]
Time: 32400[s]
Time: 43200[s]
eroded depth [m]
XB: horizontal distance [m]

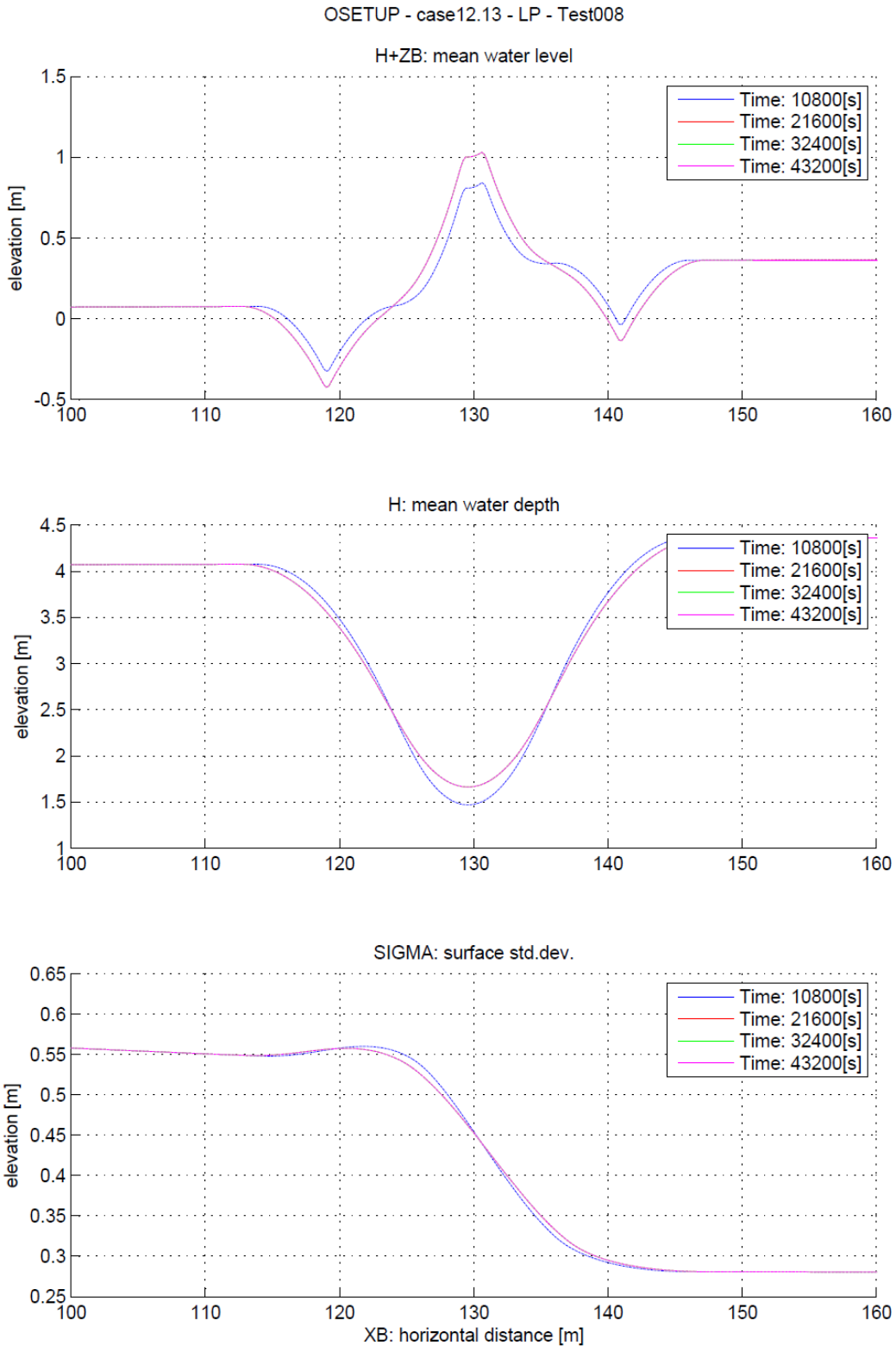
OSETUP - case12.13 - LP - Test008
H+ZB: mean water level
elevation [m]
Time: 10800[s]
Time: 21600[s]
Time: 32400[s]
Time: 43200[s]
H: mean water depth
elevation [m]
SIGMA: surface std.dev.
elevation [m]
XB: horizontal distance [m]

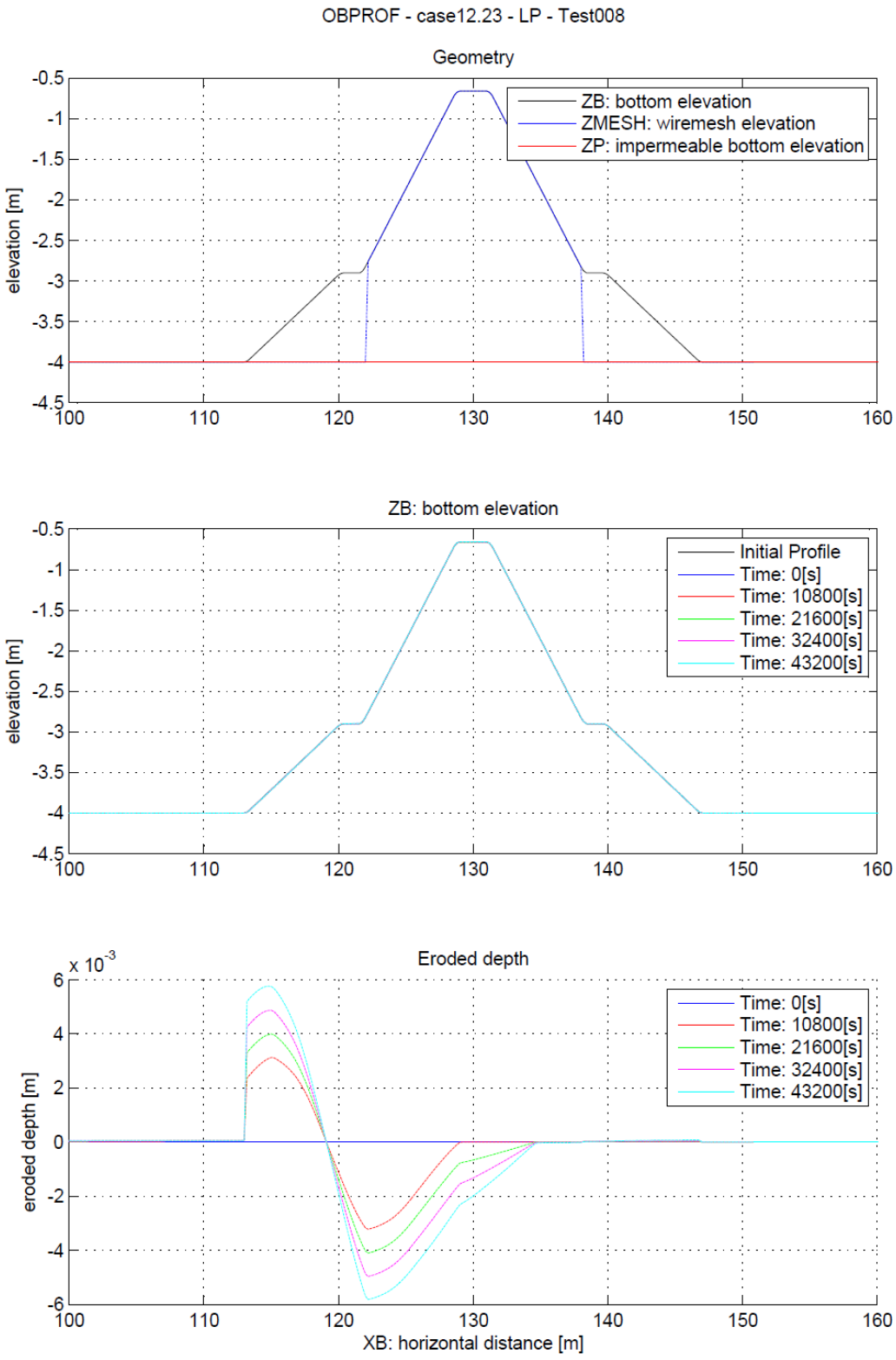
OBPROF - case12.23 - LP - Test008
Geometry
ZB: bottom elevation
ZMESH: wiremesh elevation
ZP: impermeable bottom elevation
elevation [m]
ZB: bottom elevation
Initial Profile
Time: 0[s]
Time: 10800[s]
Time: 21600[s]
Time: 32400[s]
Time: 43200[s]
elevation [m]
Eroded depth
x 10^-3
Time: 0[s]
Time: 10800[s]
Time: 21600[s]
Time: 32400[s]
Time: 43200[s]
eroded depth [m]
XB: horizontal distance [m]